Rewritable Surface on a Plastic Substrate Using Fluorous Affinity

Tsuchii, Takane
Kaneko, Kazuki
Morita, Kenta
Nishino, Takashi
Maruyama, Tatsuo

(Citation)
ACS Applied Materials & Interfaces,14(2):3255-3263

(Issue Date)
2022-01-19

(Resource Type)
journal article

(Version)
Accepted Manuscript

A rewritable surface on a plastic substrate using fluorous affinity

*Takane Tsuchii,[†] Kazuki Kaneko,[†] Kenta Morita,[†] Takashi Nishino,[†] Tatsuo Maruyama[†,‡,]**

[†] Department of Chemical Science and Engineering, Graduate School of Engineering, Kobe University, 1-1 Rokkodai, Nada-ku, Kobe 657-8501, Japan.

[‡] Research Center for Membrane and Film Technology, Kobe University, 1-1 Rokkodai, Nada, Kobe 657-8501, Japan

KEYWORDS. Fluoropolymer, micropatterning, erasable surface function, surface immobilization, surface segregation

ABSTRACT. Fluorous chemistry has unique features and high potential applicability, which are distinct from those of nonfluorinated organic compounds. However, there are limited reports detailing the applications of fluorous–fluorous interactions (fluorophilicity or fluorous affinity), likely because these interactions are not found in nature. In the present study, we describe the rewritable surface functionalization of a plastic substrate based on fluorous affinity. Plastic substrates were dip-coated with a series of methacrylate-based fluoropolymers to generate fluorous surfaces. Fluorous-tagged small molecule (perfluoroalkyl (Rf) amines) were immobilized on the fluorous surfaces via fluorous–fluorous interactions, thereby introducing reactive functional

groups (amino moieties) on the surface. The amino groups displayed on the surface (accessible by a reactant) were successfully quantified using a reactive fluorophore, which enabled quantitative analysis of the Rf-amines immobilized on the fluorous surface that were available for the subsequent reaction. The effect of the molecular structures of the fluoropolymers and Rf-amines on the surface immobilization of Rf-amines were also investigated quantitatively. The surface coated with a fluoropolymer containing $–C_8F_{17}$ most effectively immobilized an Rf-amine comprising two $–C_6F_{13}$ chains. The adhered Rf-amines were easily removed by washing the surface with methanol, and then, they could successfully be re-immobilized on the surface. Finally, the presented approach enabled the rewritable micropatterning of an Rf-tagged biomolecule on a plastic surface through microcontact printing.

1. INTRODUCTION

Surface functionalization of inexpensive bulk materials represents a rational approach for producing multifunctional devices and adding value to inexpensive bulk materials because it exploits the mechanical characteristics of the bulk materials and creates tailored functional properties on the surfaces. A commodity plastic substrate comprises a wide variety of plastics that exhibit properties that make them advantageous bulk materials, including plasticity, light-weight, disposability, tunable transparency, and compatibility with other polymers. These characteristics lead to safe and disposable diagnostic devices, portable analytical devices, and replaceable separation/adsorption units. To date, numerous methods have been developed for functionalizing the surfaces of plastic substrates.[1-6] For example, coating a plastic surface with a functional polymer solution is one of the most practical and simple strategies. In many cases, a functional polymer is more expensive than a commodity plastic. Coating with a functional polymer solution

can functionalize the surfaces of substrates with various shapes and sizes, and can minimize the usage of the functional polymer, which does not affect the mechanical characteristics of a substrate. Our group previously studied plastic substrates dip-coated with a functional polymer solution and succeeded in introducing reactive groups on the outermost surface.[7-10] However, surface functionalization based on the dip-coating approach is irreversible and not well suited for micropatterning without lithography. Reversible surface functionalization is generally termed "rewritable",[11-15] and this process can enable erasable information storage and reduce plastic wastes. Micropatterning without lithography allows for surface functionalization of designated surface areas of objects with complicated structures.

Rewritable surface functionalization based on fluorous chemistry represents one potential way to overcome these challenges. Perfluorinated organic compounds, especially those containing perfluoroalkyl groups (Rf groups), seem to have attractive interactions with other perfluorinated organic compounds in water and organic solvents due to the decreased interaction between perfluorinated compounds and other (solvent) molecules. These interactions are known as fluorophilicity,[16, 17] fluorous affinity or fluorous–fluorous interactions, and they have been exploited for liquid phase separations using a fluorous phase,[18-20] organic synthesis with facile product/catalyst separation,[21, 22] fluorous affinity columns,[23, 24] and surface immobilization of various fluorous-tagged molecules.[25-31] In general, an Rf group is chemically stable, and a surface functionalized with Rf groups exhibits inert and low-fouling properties.[9, 32, 33]

Several studies have described the immobilization of fluorous-tagged molecules on fluorous surfaces using fluorous–fluorous interactions as non-covalent linkages.[25-31, 34-37] Interestingly, the Spring and Clark groups demonstrated the facile removal of surface-bound fluorous-tagged molecules via simple solvent washing.[34, 35] Most of these studies report the successful preparation

of glass-based microarrays using fluorous–fluorous interactions, which were evaluated for qualitative assays. To our knowledge, quantitative investigations regarding the immobilization of fluorous-tagged molecules on a fluorous surface have not yet been conducted.

In the present study, a plastic substrate was dip-coated with a fluoropolymer solution to prepare a fluorous surface (Figure 1). A series of methacrylate-based fluoropolymers and Rf-amines were synthesized for this purpose. Rf-amines were immobilized on the fluorous surface to introduce reactive functional groups (amino groups) on an inert (fluorous) surface. The amino groups on the surface were quantified using a reactive fluorophore, and the effects of the molecular structures of the fluoropolymers and Rf-amines on the surface immobilization of Rf-amines were investigated. Finally, rewritable micropatterning of an Rf-tagged biomolecule was successfully performed on a fluorous surface using microcontact printing (μCP).

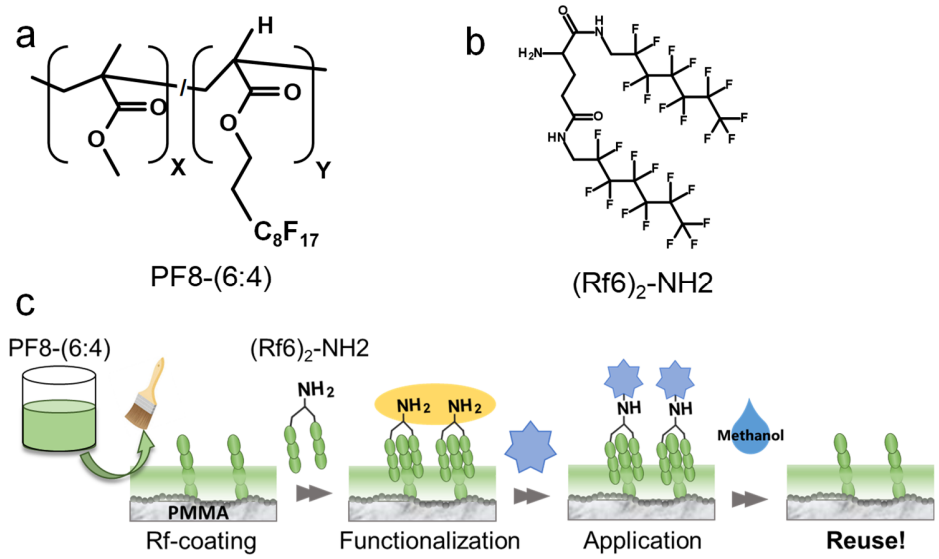

Figure 1. a, b) Chemical structures of a random fluorocopolymer (PF8-(6:4)) synthesized and a perfluoroalkyl (Rf) amine ($(Rf6)_2$-NH_2). c) Schematic illustration of a rewritable surface using fluorous affinity.

2. EXPERIMENTAL

Materials

Materials, synthesis of Rf-amines and characterization results are provided in the Supporting Information (Tables S1-S2; Figures S1-S15; Schemes S1-S3).

Polymerization of fluorocopolymers (PF8-(X:Y), PF6-(6:4), and PF4-(6:4)).

Free-radical polymerization was performed to synthesize random fluorocopolymers containing Rf groups. For example, MMA, 2-(perfluorooctyl)ethyl acrylate (PFEA8), and AIBN (0.5 wt.% relative to the total monomer weight) were dissolved in ethyl acetate and stirred at 70 °C overnight in a glass vial to prepare (PF8-(X:Y) (Figure 1a), where X and Y represent the monomer compositions. The quantities of each reagent used for the polymerization are summarized in Table S1. Each reaction solution was poured into excess *n*-hexane to precipitate the copolymer, which was then washed twice with excess *n*-hexane. The copolymer was then dried at 50 °C overnight under vacuum. Poly(MMA-*r*-PFEA6) (PF6-(6:4)) and poly(MMA-*r*-PFEA4) (PF4-(6:4)) were also synthesized in a similar manner, where PFEA4 and PFEA6 represent 2-(perfluorobutyl)ethyl acrylate and 2-(perfluorohexyl)ethyl acrylate, respectively. Table S2 summarizes the number-averaged molecular weights (*Mn*) and polydispersity indices (*M*w/*M*n) of PF*n*-(6:4).

Characterization

Proton nuclear magnetic resonance (^{1}H-NMR) analysis was performed using an Avance-500 (Bruker BioSpin GmbH, Rheinstetten, Germany) in chloroform-*d* solvent containing 0.03 wt.% tetramethylsilane as an internal standard. The ^{1}H-NMR results are presented in Figures S1–S7.

The weight-averaged molecular weight (*M*w) and number-average molecular weight (*M*n) were measured using a size exclusion chromatograph (SEC; LC-2000 plus, JASCO, Tokyo, Japan) equipped with a 7.5 × 300 mm SEC column (GF510, Showa Denko K.K., Tokyo, Japan) and a refractive index detector (RI-8031, JASCO, Tokyo, Japan) at 40 °C using tetrahydrofuran (THF) as an eluent. Poly(methyl methacrylate) was used for the molecular weight standards. The molecular weights and polydispersity of the synthesized copolymers are compiled in Table S1 in the main text. The densities of the copolymers were measured using a sink-float density determination method.

Dip-coating of PF8-(X:Y) on an acrylic (PMMA) substrate

PMMA substrates were dip-coated in a copolymer solution, and perfluoroalkyl (Rf) groups were introduced on the outermost surface of the substrate using the following procedure. A PMMA substrate (0.5-mm-thick) was cut into 1 cm × 1 cm pieces. PF8-(X:Y) was dissolved in ethyl acetate to prepare a 1 wt.% copolymer solution. A PMMA substrate (1 cm × 1 cm) was immersed in the copolymer solution for a few seconds and withdrawn from a solution over 3 s. The PMMA substrate was then dried at room temperature overnight under vacuum.

Contact angle measurements using water and oil droplets were performed using a digital automated contact angle goniometer DMs-401 (Kyowa Interface Science Co., Ltd., Niiza, Japan) at room temperature. Water and oil (*n*-hexadecane) droplets were 5 μL.

X-ray photoelectron spectroscopy (XPS) measurements were performed using a PHI X-tool X-ray photon spectrometer (ULVAC, Chigasaki, Japan) using an Al Kα source (15 kV, 48 W). To obtain wide spectra, the photoelectron take-off angle was 45°, and the spot size was 199 μm × 199 μm. Survey scans were performed with a pass energy of 280 eV and a step size of 1.0 eV. Depth profiling was performed using an Ar^+ source at 4.00 keV; the scanning range was 699.0–679.0 eV (step size = 0.25 eV), and the sputtering was carried out in one-minute intervals for a total of 40 min.

Field-emission scanning electron microscopy (FE-SEM) observations were performed using a JSM-7500F field-emission scanning electron microscope (JEOL, Tokyo, Japan) (Figure S8). All SEM images were collected at an acceleration voltage of 7 kV and an emission current of 100 μA.

Immobilization of Rf-amines and quantification of surface-displayed amino groups

As an example, Rf8-NH_2 was dissolved in a solvent mixture (DMSO:methanol:water = 2:2:1 volume ratio) to prepare a solution containing 1.0 mM Rf8-NH_2. Dip-coated substrates were immersed in 2 mL of the Rf8-NH_2 solution, followed by gentle shaking for 1.5 h at room temperature. The substrates were withdrawn from the solution and dried at 50 °C for 4 h under vacuum. The substrates were washed with an excess amount of water and floated on a 0.75-mL phosphate buffer solution (50 mM, pH 7.8) containing 0.1 mM sulfo-Cy5-NHS ester, followed by gentle shaking for 4 h at room temperature. The substrates were washed with phosphate buffer (0.1 M, pH 7.8) three times and immersed in fresh phosphate buffer (2 mL), followed by gentle shaking for 1 h. The substrates were then immersed in methanol (2 mL) and shaken for 1 h to liberate Cy5-tagged Rf8-NH_2 from the substrate surfaces. The fluorescence intensity (excitation at 646 nm,

emission at 662 nm) of the methanol containing Cy5-tagged Rf8-NH_2 was measured using a fluorescence spectrophotometer (FP-8200, JASCO, Tokyo, Japan). The measurements were repeated three times and the data were averaged and the results presented with error bars (standard deviations).

While the above procedure employed 0.1 mM sulfo-Cy5-NHS ester, sulfo-Cy5-NHS ester at higher concentrations (0.2 mM and 0.4 mM) was also used for the quantification of the surface-displayed amino groups. There was no obvious difference in the quantification among these concentrations of sulfo-Cy5-NHS ester, indicating that 0.1 mM sulfo-Cy5-NHS ester was sufficient for the quantification.

Rewriting on a PF8-(6:4)-coated surface

The PF8-(6:4)-coated substrate was evaluated to test the rewritability of the system using fluorous–fluorous interaction. The writing procedure (i.e., $(Rf6)_2$-NH_2 immobilization, Figure 1b) and the removal procedure (i.e., washing out $(Rf6)_2$-NH_2, Figure 1c) were repeated. The writing procedure was carried out as follows. The PF8-(6:4)-coated substrate was immersed in 2 mL of $(Rf6)_2$-NH_2 solution (1 mM, in a DMSO/methanol/water mixture) and shaken for 1.5 h at 25 °C. The substrate was dried at 50 °C for 4 h. The substrate was washed with excess water and dried under vacuum. The substrate was floated on 0.10 mM sulfo-Cy5-NHS ester solution (0.75 mL) and shaken for 4 h at room temperature. The substrate was washed with phosphate buffer three times and immersed in a fresh phosphate buffer solution (2 mL) and shaken for 1 h.

The removal procedure was carried out as follows. The substrate obtained by the procedure described above was immersed in 2 mL of a methanol/water mixture (3:1 volume ratio) and shaken

for 1 h to cleave the fluorous–fluorous interactions. The substrate was then immersed in 2 mL of an aqueous solution containing 1 wt.% sodium dodecyl sulfate (SDS) for 1 min, and then washed with water and a methanol/water mixture three times. The substrate was finally immersed in 2 mL of a methanol/water mixture (3:1 volume ratio), shaken for 30 min at room temperature, and dried under vacuum.

Microcontact printing of $(Rf6)_2$-biotin

To prepare a polydimethylsiloxane (PDMS) stamp, a SYLGARD™ 184 Silicone Elastomer Kit (Dow Inc., Midland, MI) was employed. The base and curing agents were mixed in a 10:1 mass ratio, and the mixture was added to an aluminum stamp mold. After degassing under vacuum, the mixture and mold were heated to 80 °C in an oven. The PDMS stamp was removed from the mold and cut into 1-cm squares (Figure S15).

$(Rf6)_2$-biotin was dissolved in methanol to prepare a 10 mM solution. The $(Rf6)_2$-biotin solution (20 μL) was applied to the PDMS stamp and dried for 1 h at room temperature. The PDMS stamp was placed on the PF8-(6:4)-coated surface, and a 50-g weight was placed on the PDMS stamp for 30 min. The stamped substrate was then washed with an excess amount of water three times and dried under vacuum. A Streptavidin Fluor™ 488 conjugate solution (30 μL, 10 μg/mL, in 50 mM phosphate buffer pH 7.4) was put on the stamped substrate surface and incubated for 5 min. The substrate was washed with an excess amount of water three times. The substrate surface was observed using a confocal laser scanning microscope (CLSM; Fluoroview FL3000, Olympus, Tokyo, Japan). To remove the $(Rf6)_2$-biotin/streptavidin complex, the substrate was immersed in 2 mL of an aqueous solution containing 1 wt.% SDS for 1 min, then washed with water and

immersed in 2 mL of a methanol/water solution (3:1 volume ratio) for 30 min at 25 °C three times. After vacuum drying, the microcontact printing procedure followed by the removal using a methanol/water solution was repeated twice more.

3. RESULTS & DISCUSSION

3.1 Contact angle measurements of dip-coated acrylic surfaces

Random fluorocopolymers, termed PF8-(X:Y), with various monomer compositions were synthesized using methyl methacrylate (MMA) and 2-(perfluorooctyl)ethyl acrylate (PFEA8) as monomers (Figure 1). The monomer ratio of X to Y (i.e., MMA:PFEA8) in the reaction ranged from 10:0 to 5:5. ^{1}H-NMR analysis revealed that the monomer ratios in the products were very close to those in the reaction, as shown in Table 1. The number-averaged molecular weights (Mn) and polydispersity indices (Mw/Mn) of the copolymers are also summarized in Table 1. Many copolymers were successfully synthesized with Mn greater than 3×10^4. However, the PF8-(5:5) gave an Mn of only 1.9×10^3. In general, a high content of Rf groups in a polymer decreases its solubility in a non-halogenated solvent and also promote the self-folding of a polymer,[38-40] which resulted in the small molecular weight in the synthesis of PF8-(5:5). A PMMA substrate was dip-coated with an ethyl acetate solution containing PF8-(X:Y) to introduce Rf groups on the outermost surface. For example, the weight change of an acrylic substrate following dip-coating in PF8-(6:4) indicated that the thickness of the dip-coated layer was approximately 0.4 μm based on the density of PF8-(6:4) (1.46 g/cm^3) (see Supporting Information for details).

Field-emission scanning electron microscopy (FE-SEM) revealed that there was no appreciable difference between the bare and PF8-(6:4)-coated surfaces, thus indicating the successful preparation of a flat surface after dip-coating (Figure S8). The surface properties of bare and dip-

coated substrates were evaluated according to the water contact angle (WCA) (Figure 2a,c) and oil contact angle (OCA) (Figure 2b,d) analysis. The WCA on a bare PMMA surface was approximately 66°, which was consistent with previous reports.[8, 10] The WCA of PF8-(X:Y)-coated surfaces increased according to the increase in the proportion of PFEA8 monomer in the copolymer; WCAs of surfaces coated with PF8-(6:4) and PF8-(5:5) were both about 114°, indicating that these surfaces were highly hydrophobic. The OCA measurements were also performed on the substrates using *n*-hexadecane. The OCA of the bare PMMA surface was about 13°, which was typical for a PMMA surface,[41, 42] and the OCA of PF8-(X:Y)-coated surfaces also increased according to the increase in the proportion of PFEA8 in the copolymer. The OCAs of surfaces coated with PF8-(6:4) and PF8-(5:5) were about 76°, meaning that the surfaces were oil-repellent. These high WCAs and OCAs suggested that Rf groups were introduced on the outermost surfaces of the substrates following the dip-coating process. In addition, as the monomer ratio of PFEA8 increased in the copolymer, the quantity of Rf groups present on the surface increased; the large contact angles of water and oil droplets confirmed the high composition of Rf groups on the outermost surface.

Table 1. Number-average molecular weights (*M*n) and polydispersity indices (*M*w/*M*n) of PF8-(X:Y).*

Polymer	Monomer ratio in a product	*M*n	*M*w/*M*n
PF8-(9:1)	94:6	4.6×10^4	1.5

PF8-(8:2)	85:15	6.9×10^4	1.5
PF8-(7:3)	73:27	5.5×10^4	1.4
PF8-(6:4)	58:42	3.1×10^4	1.4
PF8-(5:5)	51:49	1.9×10^3	1.2

*Mn and Mw/Mn were determined by size-exclusion chromatography.

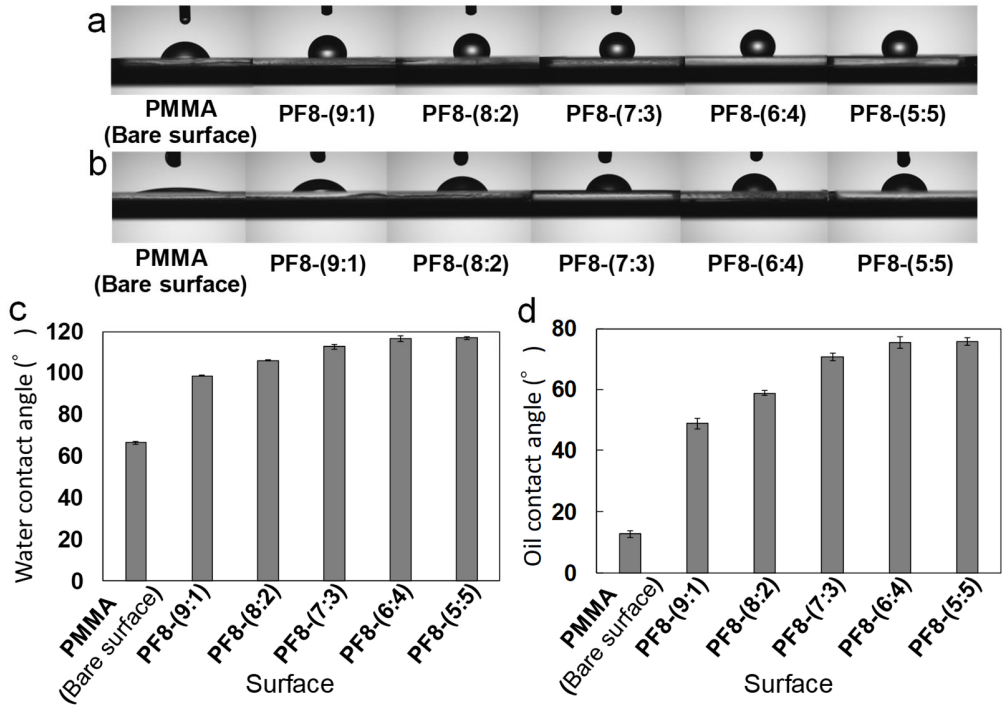

Figure 2. Optical images of (a) water and (b) oil contact angles on substrate surfaces, and charts depicting the (c) water and (d) oil contact angles on substrate surfaces.

3.2 X-ray photoelectron spectroscopy analysis of dip-coated PMMA surfaces

X-ray photoelectron spectroscopy (XPS) analysis of bare and PF8-(6:4)-coated surfaces was performed (Figure 3a,b). The O1s and C1s peaks (at 531 eV and 285 eV, respectively) were observed on the bare PMMA surface, whereas O1s, C1s, F1s (685 eV), and F_{KLL} (832 eV) peaks were observed on the PF8-(6:4)-dip-coated surface. These results confirmed that Rf groups were displayed on the outermost surface of the PF8-(6:4)-coated substrate.

XPS depth analysis was performed for the F1s peak, and Figure 3c,d presents the XPS depth profiles of bare PMMA and PF8-(6:4)-dip-coated substrates. No discernable peak was observed around 685 eV on the bare PMMA surface, even after Ar^+ sputtering for 40 min. When the PF8-(6:4)-coated surface was sputtered with Ar^+, an F1s peak was observed in the first minute, but no peak was observed during the remaining sputtering time. These results suggested that Rf groups were segregated to the outermost surface of the substrate, likely because the Rf groups preferentially minimize the surface energy at the air-polymer interface.[8, 43-45]

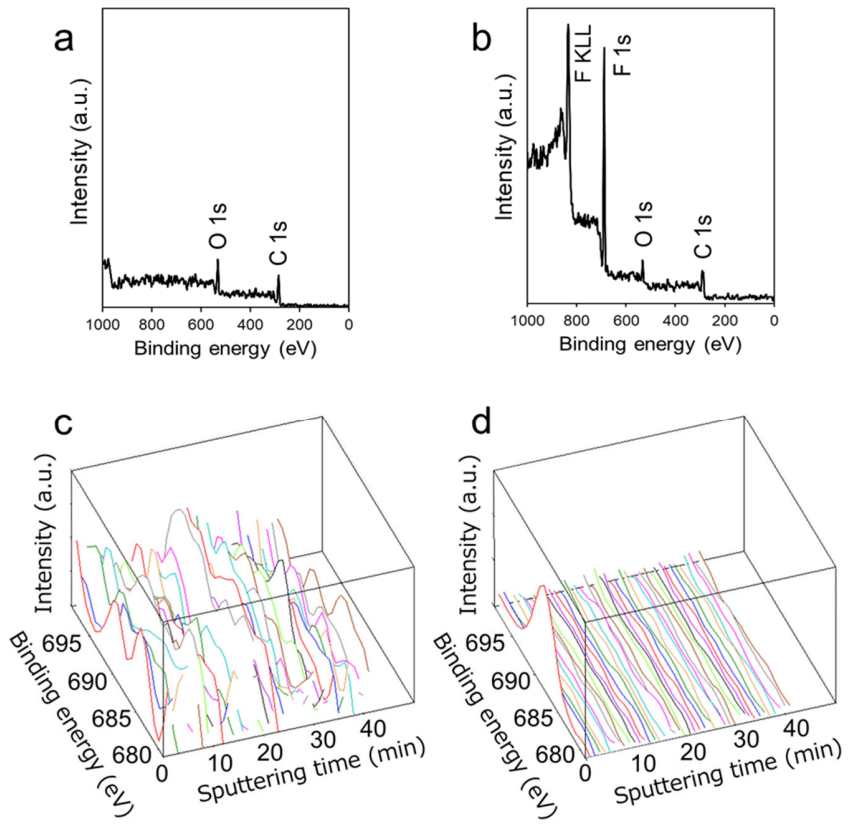

Figure 3. XPS spectra of (a) bare PMMA and (b) PF8-(6:4)-coated PMMA substrate surfaces; XPS depth profiles of (c) bare PMMA and (d) PMMA coated with PF8-(6:4).

3.3 Immobilization of an Rf-tagged small molecule on dip-coated surfaces via fluorous affinity

To demonstrate a fluorous−fluorous interaction on the PF8-(6:4)-coated surface, an Rf-tagged small molecule, C_8F_{17}-CH_2-NH_2 (Rf8-NH_2), was immobilized on the PF8-(6:4)-coated surface. Following the immobilization of Rf8-NH_2, the surface-bound amino groups of Rf8-NH_2 were conjugated with a reactive fluorophore (sulfo-Cy5 NHS ester), and the Cy5-tagged Rf8-NH_2 was then liberated into methanol. The amount of fluorophore liberated in methanol was quantified

using a fluorescence spectrophotometer to deduce the amount of Rf8-NH_2 immobilized on the surfaces. In general, a reaction yield on a solid surface using a dissolved reactant does not reach 100% because of several factors (steric hindrance, repulsive interaction, surface-specific microenvironment etc).[46] In the present study, amino groups reacted on the surface represented the amino groups that were accessible by a reactant in solution. The amount of the accessible amino groups was regarded as the amount of the immobilized Rf-tagged small molecule that were available for the subsequent reaction. A schematic diagram illustrating the immobilization of Rf8-NH_2 and its quantification is presented in Figure 4a.

Figure 4b shows the amount of fluorophore immobilized on the analyzed substrate surfaces. A negligible amount of the fluorophore was adsorbed on the bare and dip-coated surfaces without Rf8-NH_2, and a relatively small amount of the fluorophore was observed on the bare PMMA surface with Rf8-NH_2. However, significant amounts of fluorophore were detected on the dip-coated surfaces with immobilized Rf8-NH_2. As the monomer ratio of MMA:PFEA8 increased from 9:1 to 6:4, the amount of immobilized fluorophore also increased, but a monomer ratio of 5:5 resulted in a slightly decreased amount of immobilized fluorophore. The largest amount of fluorophore (≈ the amount of Rf8-NH_2) was immobilized on the surface coated with PF8-(6:4).

To clarify the importance of fluorous–fluorous interactions for the immobilization on the PF8-(6:4)-coated surface, 1-octylamine was used as an alternative to Rf8-NH_2. Sulfo-Cy5-NHS-ester was conjugated to 1-octylamine immobilized on the surface. Fluorescence measurements revealed that there was a negligible amount (<0.3 pmol/cm^2) of the fluorophore immobilized on the PF8-(6:4)-coated surface. These results indicated that the fluorous–fluorous interactions were essential for the immobilization of an Rf-tagged small molecule on a fluorous surface, and furthermore, PF8-(6:4) was an optimal coating polymer for the immobilization of Rf-tagged small molecules.

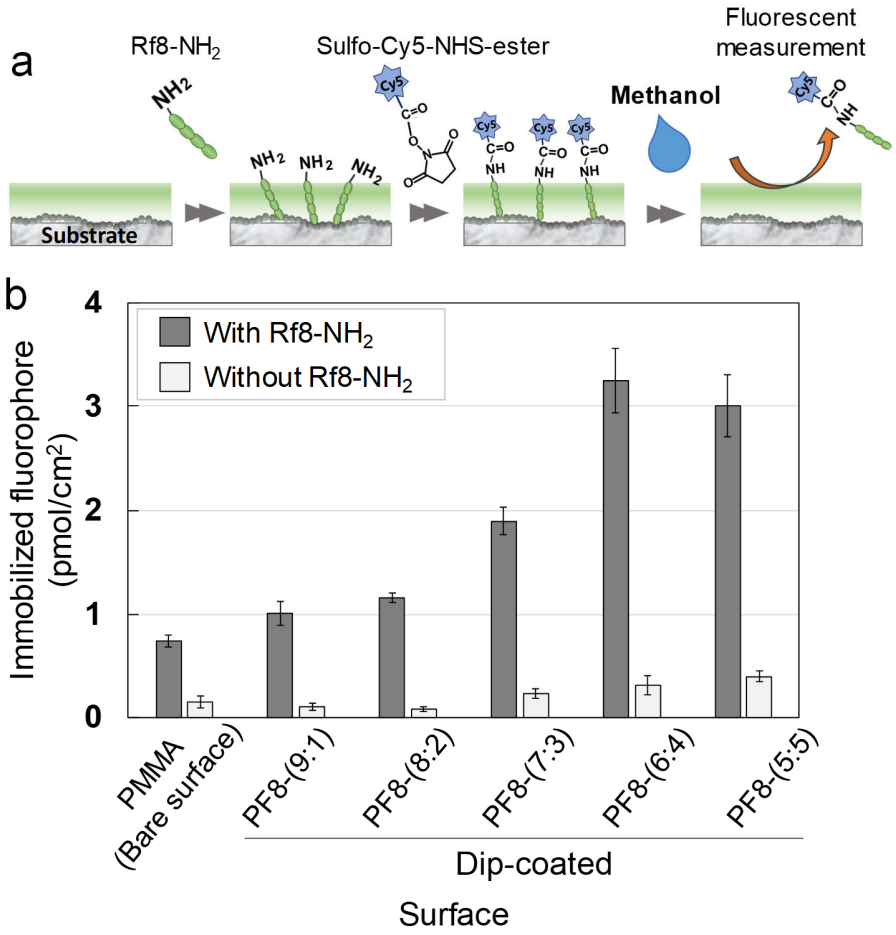

Figure 4. (a) Schematic illustration of the immobilization of Rf8-NH_2 on a fluorous surface and the quantification of surface-bound Rf8-NH_2; (b) quantities of sulfo-Cy5-NHS-ester immobilized on PF8-(X:Y)-coated surfaces with and without Rf8-NH_2.

3.4 Effect of the Rf-amine's molecular structure on its surface immobilization

To effectively immobilize Rf-amines on the dip-coated surface, Rf-amines with various molecular structures were investigated. Four distinct Rf-amines were prepared to evaluate the interactions between Rf-amines and the PF8-(6:4)-dip-coated surface (Figure 5a). Specifically,

Rf6-NH_2 had a single Rf chain and a carbon chain length of six; Rf8-NH_2 had a single Rf chain and a carbon chain length of eight; $(Rf4)_2$-NH_2 had two Rf chains, each with a carbon chain length of four; $(Rf6)_2$-NH_2 had two Rf chains, each with a carbon chain length of six. These Rf-amines were immobilized on the PF8-(6:4)-coated surface via fluorous–fluorous interactions, and the immobilized Rf-amines were quantified using a reactive fluorophore following the procedure described above. The quantity of the immobilized fluorophore was considered to represent the amount of Rf-amines in the experiments discussed below.

Figure 5b shows the amounts of Rf-amines immobilized on the studied surfaces. A bare PMMA surface immobilized a relatively small amount of Rf-amines except for $(Rf6)_2$-NH_2; the considerable amount of $(Rf6)_2$-NH_2 was likely immobilized on the bare PMMA surface through nonspecific adsorption, probably because of its high hydrophobicity and its low solubility in water. There were negligible quantities of the fluorophores adsorbed on the PF8-(6:4)-coated substrate without an Rf-amine, thus highlighting the low-fouling properties of the PF8-(6:4)-coated surface. Several reports have demonstrated that fluorinated surfaces exhibit low-fouling properties.[9, 47, 48] The fluorinated surface prepared in the present study also showed low adsorption of organic compounds. However, remarkable amounts of the Rf-amines were immobilized on the PF8-(6:4)-coated surface. In particular, $(Rf4)_2$-NH_2 and $(Rf6)_2$-NH_2 were immobilized at greater than 6 pmol/cm^2. The presence of two Rf chains in these compounds seemed to enhance their interactions with the fluorinated surface, while the amide bonds in the $(Rf4)_2$-NH_2 and $(Rf6)_2$-NH_2 reduced their water solubility, which might also help the immobilization. $(Rf6)_2$-NH_2 was immobilized in the largest amount on the PF8-(6:4)-coated surface. These results suggest that Rf6- was more effective than Rf4- in terms of immobilization on the fluorous surface. Overall, it was concluded

that the number and length of Rf chains played a significant role in their surface immobilization based on fluorous affinity.[49, 50]

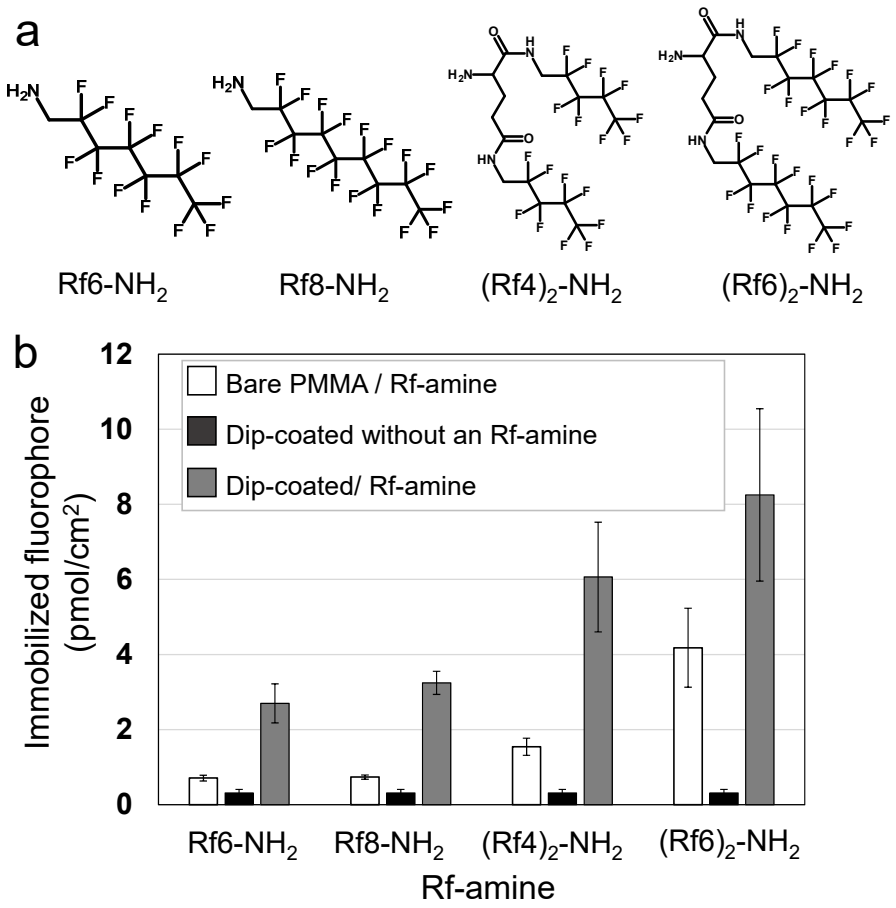

Figure 5. (a) Chemical structures of Rf-amines used in this study; (b) amounts of sulfo-Cy5-NHS-ester immobilized on PF8-(6:4)-coated surfaces with and without Rf-amines.

XPS N1s (~400 eV) depth analysis was performed for the PF8-(6:4)-coated surfaces with immobilized Rf-amines (Figure 6). The N1s peaks were ambiguous on the PF8-(6:4)-coated surfaces with immobilized Rf6-NH_2, Rf8-NH_2, and $(Rf4)_2$-NH_2 (Figure 6a, 6b, and 6c,

respectively) although the investigations described above using the fluorophore indicated the presence of these amino groups on the substrate surfaces. In general, the XPS detection sensitivity for N1s is relatively lower than for F1s.[7] The N1s peak was clearly observed on the outermost surface of the PF8-(6:4)-coated substrate with immobilized $(Rf6)_2$-NH_2. The possible reasons why the high intensity of N1s was observed only on the PF8-(6:4)-coated substrate were the relatively large amount of $(Rf6)_2$-NH_2 molecules immobilized on the surface and their molecular orientation on the surface. The amino groups of the immobilized $(Rf6)_2$-NH_2 molecules might point toward the bulk substrate due to fluorous–fluorous interaction; therefore, the amino groups might be oriented outward, enhancing the intensity of N1s. However, there are still uncertainties on the control of molecular orientation on the surface.

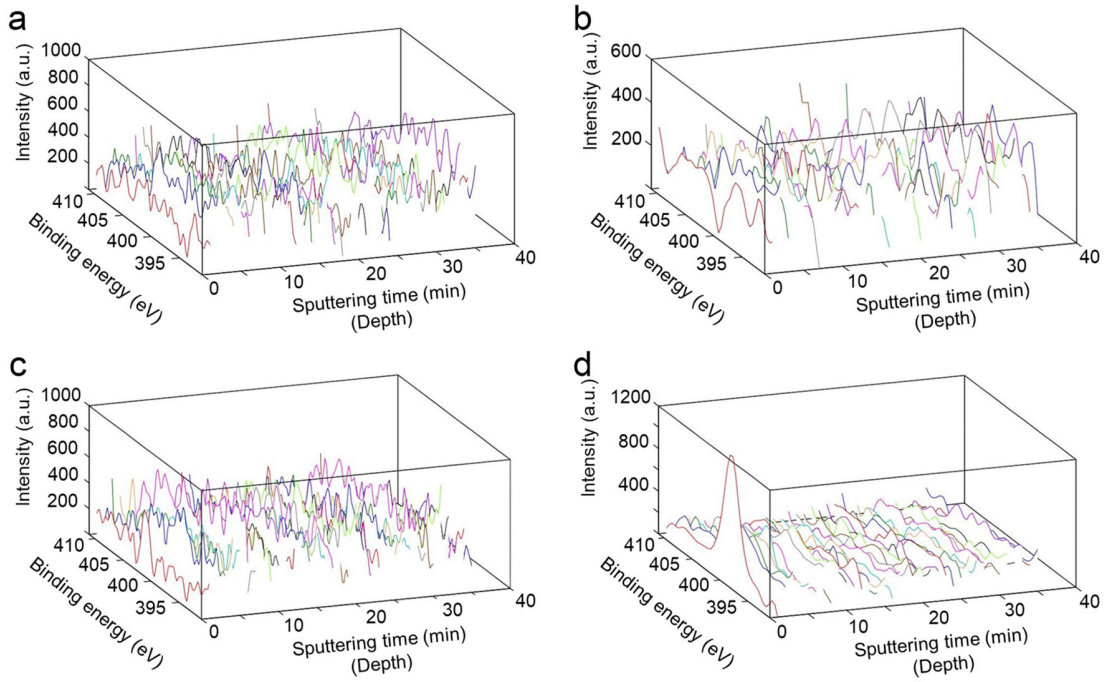

Figure 6. XPS N1s depth profiles of PF8-(6:4)-coated surfaces that immobilized Rf-amines: (a) $Rf6$-NH_2; (b) $Rf8$-NH_2; (c) $(Rf4)_2$-NH_2; (d) $(Rf6)_2$-NH_2.

3.5. Effect of the Rf groups in the fluoropolymer on the immobilization of Rf-amines

The effect of the chain length of the Rf groups in the fluoropolymer on the immobilization of Rf-amines was investigated. Fluoropolymers with various Rf group chain lengths were synthesized for this purpose (PF#; Figure 7a, Table S2). The monomer composition (MMA:Rf-acrylate) was set at 6:4, and PMMA substrates were dip-coated with the copolymers (e.g., PF8-(6:4), PF6-(6:4), and PF4-(6:4)) before immobilizing Rf-amines on the surfaces. Again, the Rf-amines immobilized on the surfaces were quantified using a reactive fluorophore.

Figure 7b shows the amount of fluorophore immobilized on the investigated surfaces with and without Rf-amines (or octylamine). Small amounts of the fluorophore were adsorbed on bare and dip-coated substrates without Rf8-NH_2, and in the presence of Rf8-NH_2, a relatively small amount of the fluorophore was detected on the bare PMMA substrate. Large amounts of the fluorophore were immobilized on the dip-coated surfaces with Rf8-NH_2, although the amount varied according to the type of dip-coated copolymer. In particular, the PF4-(6:4)-coated surface immobilized the fluorophore at approximately 5 pmol/cm^2 in the presence of Rf8-NH_2, which was the largest among the surfaces.

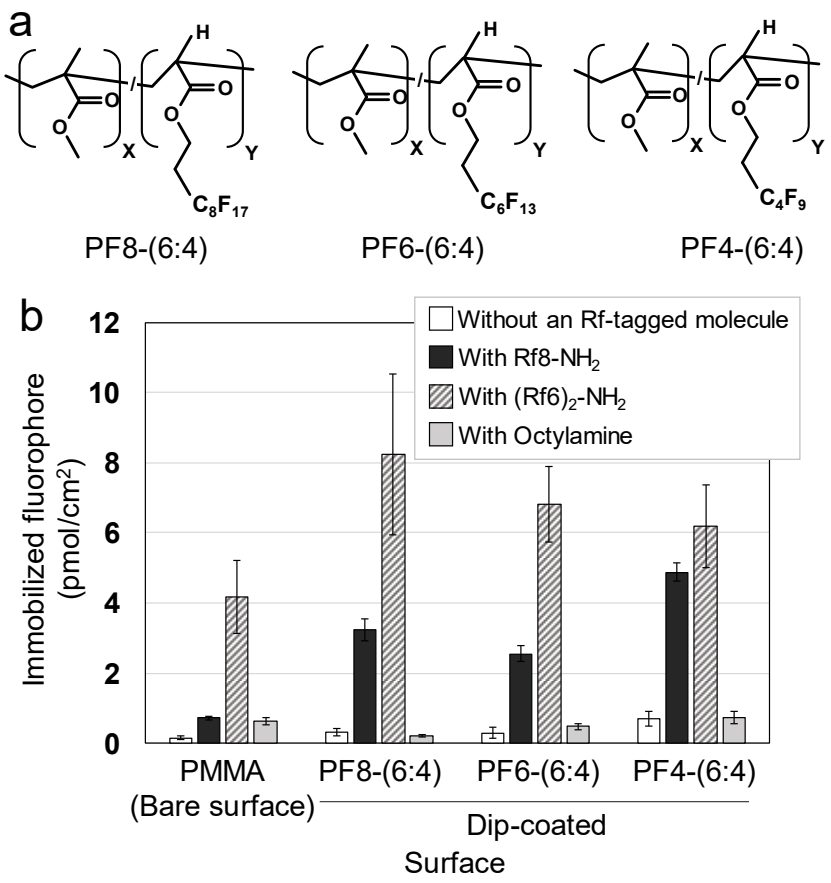

Figure 7. (a) Chemical structures of synthesized fluoropolymers; (b) amounts of sulfo-Cy5-NHS-ester immobilized on the fluoropolymer-coated surfaces with and without Rf-amines or octylamine.

In addition, $(Rf6)_2$-NH_2 was immobilized on bare and dip-coated surfaces. Significant amounts of the fluorophore were observed on the dip-coated surfaces in the presence of $(Rf6)_2$-NH_2, which were superior to those of Rf8-NH_2. The amount of fluorophore immobilized depended on the properties of the dip-coating copolymer. Unlike the results obtained with Rf8-NH_2, the PF8-(6:4)-coated surface immobilized the largest amount of fluorophore in this case (~8.2 pmol/cm^2). $(Rf6)_2$-NH_2 had two Rf groups and two amide bonds, which made $(Rf6)_2$-NH_2 highly hydrophobic. The

high hydrophobicity would also increase hydrophobic interaction in aqueous solution, probably resulting in the nonspecific adsorption of $(Rf6)_2$-NH_2 on a bare substrate. These results indicated that a large amount of $(Rf6)_2$-NH_2 was immobilized on the PF8-(6:4)-coated surface, and the amino groups of $(Rf6)_2$-NH_2 were effectively oriented toward the outermost surface, which made them available for the subsequent reaction.

A small molecule on a solid surface often migrate in the dry state. We then immobilized $(Rf6)_2$-NH_2 on the PF8-(6:4)-coated surface and left it for 1 and 5 days in the dry state. There was, however, no significant difference in the amount of amino groups displayed on the surfaces between 1 and 5 days. These results suggest that, if the migration of $(Rf6)_2$-NH_2 was, it did not affect the amount of the amino groups displayed on the surface.

Finally, *n*-octylamine was tested as an alternative to Rf8-NH_2. However, significant amounts of the fluorophore were not observed on bare or dip-coated surfaces in the presence of *n*-octylamine, indicating that *n*-octylamine did not have sufficient interactions with the surfaces (i.e., no immobilization). Fluorous–fluorous interactions derived from Rf groups therefore played an important role in the immobilization of Rf-tagged molecules on a fluorous surface.

3.6 Rewriting the function on the dip-coated surface

Fluorous–fluorous interactions can easily be cleaved using an appropriate solution (e.g., methanol or halogenated solvents).[34, 35] In this study, the removal of immobilized Rf-amines from a dip-coated surfaces was performed using methanol, and the re-immobilization of Rf-amines on the surface was evaluated. Immobilization of $(Rf6)_2$-NH_2 on the PF8-(6:4)-coated surface was carried out as described above. Then, the substrate was washed with a methanol/water mixture to

remove $(Rf6)_2$-NH_2 from the surface, and the procedure of $(Rf6)_2$-NH_2 immobilization was conducted again. Figure 8 shows the amounts of fluorophore immobilized on the PF8-(6:4)-coated surface when the $(Rf6)_2$-NH_2 immobilization and removal were repeated for three cycles. After the first immobilization and subsequent washing, only a small amount of the fluorophore (<0.9 pmol/cm^2) was immobilized on the surface, indicating the successful removal of $(Rf6)_2$-NH_2. The second immobilization of $(Rf6)_2$-NH_2 led to approximately 8 pmol/cm^2 of the fluorophore on the surface, and the second washing again resulted in a small amount of immobilized fluorophore. The third immobilization of $(Rf6)_2$-NH_2 successfully immobilized a comparable amount of fluorophore as in the previous cycles. These results demonstrate the repeatability of Rf-amine immobilization and removal on a fluorous surface based on fluorous–fluorous interactions. There observed a slight increase in the immobilization of $(Rf6)_2$-NH_2 as the immobilization and washing procedures were repeated. This increase might be explained by the further surface-segregation induced by the repetition of the procedures. The repetition of the procedures (immobilization and washing) possibly induced the further surface-segregation of Rf groups in PF8-(6:4) on the outermost surface, which rendered the surface more appropriate for the immobilization of $(Rf6)_2$-NH_2.

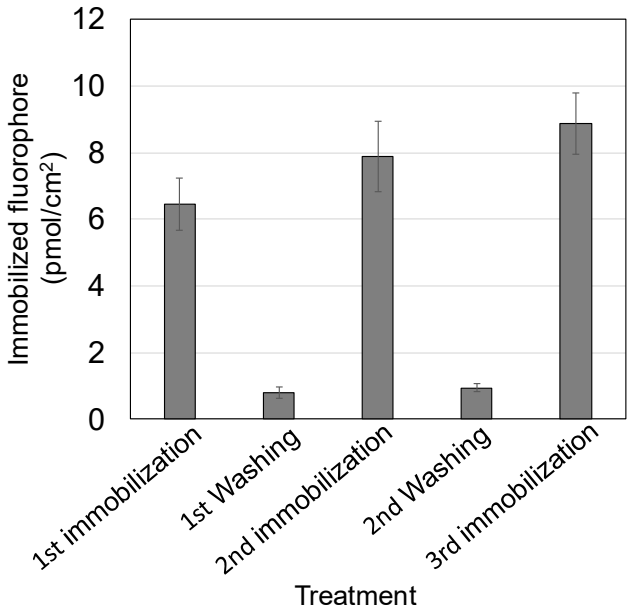

Figure 8. Repeated immobilization and removal of $(Rf6)_2$-NH_2 and quantification of amino groups on the PF8-(6:4)-coated surface.

3.7 Microcontact printing (μCP) of $(Rf6)_2$-biotin on a dip-coated surface

Finally, the μCP of biomolecules on a dip-coated surface using fluorous–fluorous interaction was investigated.[51-53] Rf-tagged biotin ($(Rf6)_2$-biotin), which had two Rf chains (Figure 9a, Scheme S3) was synthesized and used to immobilize biomolecules. A polydimethylsiloxane (PDMS) stamp (1 cm × 1 cm) was prepared with 16 small round islands (300 μm in diameter and 50 μm in height) on the surface (Figure S15), and a methanol solution containing 10 mM $(Rf6)_2$-biotin was used as ink for this stamp. After drying, the stamp was put in contact with the PF8-(6:4)-coated surface. Following washing and drying, an aqueous solution containing streptavidin Fluor™ 488 conjugate was placed on the substrate to allow the formation of the fluorescence-labeled streptavidin-biotin complex on the surface. After washing again, the surface was observed using a

confocal laser scanning microscope (CLSM). Figure 9b shows the fluorescent microscope images of the repeated μCP with $(Rf6)_2$-biotin. Each μCP process emitted green fluorescence based on the geometry of the PDMS stamp, thus indicating the successful micropatterning of $(Rf6)_2$-biotin. The μCP quality was improved with the repetition of the μCP and washing procedures, which would be the same with Figure 8.

$(Rf6)_2$-biotin had a relatively large non-fluorinated and relatively hydrophilic group (biotin), and streptavidin was successfully immobilized on the stamped area via biotin. These make us deduce that a biotin group in $(Rf6)_2$-NH_2 was oriented outward when it was immobilized on the fluorous surface. There was a small amount of green fluorescence from areas other than the stamped sites after each μCP step, which means that nonspecific adsorption of streptavidin was suppressed. The micropatterning was clearly removed after washing with methanol, and the repetition of μCP successfully gave the micropatterning of $(Rf6)_2$-biotin again.

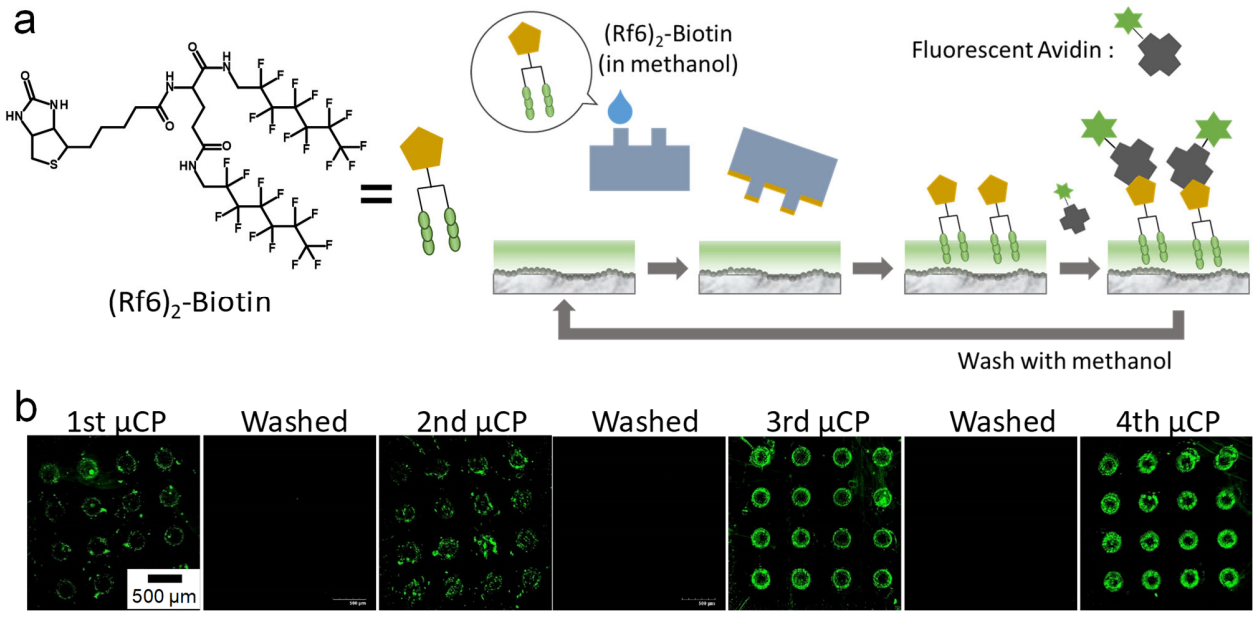

Figure 9. Microcontact printing of $(Rf6)_2$-biotin via fluorous affinity. (a) Schematic illustration of the μCP of $(Rf6)_2$-biotin using fluorous affinity and biotin-streptavidin affinity. (b) CLSM images of repeated μCP of $(Rf6)_2$-biotin followed by staining using fluorescence-labeled streptavidin.

4. CONCLUSIONS

In the present study, rewritable surface functionalization of a plastic substrate was achieved by taking advantage of fluorous affinity. The surface of a plastic substrate was dip-coated with a series of methacrylate-based fluoropolymers containing Rf groups. Then, Rf-amines were successfully immobilized on the fluorous surfaces through fluorous–fluorous interactions, thereby introducing reactive functional groups (amino moieties) on the fluorous surface. Quantification of the surface-displayed amino groups using a reactive fluorophore enabled quantitative evaluations of Rf-amines immobilized on each substrate surface. These investigations revealed that a surface coated with a fluoropolymer containing $–C_8F_{17}$ most effectively immobilized an Rf-amine having two chains of $–C_6F_{13}$. The immobilized Rf-amines were easily removed from the surface by washing with methanol, and they could then successfully be re-immobilized on the surface. Finally, the developed approach allowed for rewritable micropatterning of a biomolecule on a plastic surface using μCP. The fluorous chemistry on a fluorous surface has a high potential in the reversible control of surface properties of plastic objects, which will open the application of fluorous chemistry to analytical device and an information storage technology.

ASSOCIATED CONTENT

Supporting Information. Materials, Experimental details and Supplementary Results. This material is available free of charge via the Internet at http://pubs.acs.org.

Experimental, H NMR charts, MALDI-TOF/MS charts and FE-SEM images.

AUTHOR INFORMATION

Corresponding Author

tmarutcm@crystal.kobe-u.ac.jp

ORCID

Tatsuo Maruyama: 0000-0003-2428-1911

Notes

The authors declare no competing financial interest.

Author Contributions

Study conception and design: T. T. and T. M. Experiments, analysis and interpretation of results: T. T., K. M. and T. N. Manuscript preparation: T.T. and T. M. All authors reviewed the results and approved the final version of the manuscript.

Funding Sources

This study was financially supported by JSPS KAKENHI Grant Numbers 21K18850, 20H02542, 20H04711 and 19H05458, and also by Iketani Science and Technology Foundation. This study was partially supported by Takeda Science Foundation.

ACKNOWLEDGMENT

The authors thank Prof. A. Kondo for their technical help with MALDI-TOF/MS. The authors thank Edanz (https://jp.edanz.com/ac) for editing a draft of this manuscript.

REFERENCES

1. Denes, F. S.; Manolache, S., Macromolecular Plasma-Chemistry: An Emerging Field of Polymer Science. *Prog. Polym. Sci.* **2004,** *29* (8), 815-885.

2. Love, J. C.; Estroff, L. A.; Kriebel, J. K.; Nuzzo, R. G.; Whitesides, G. M., Self-Assembled Monolayers of Thiolates on Metals as a Form of Nanotechnology. *Chem. Rev.* **2005,** *105* (4), 1103-1169.

3. Lahann, J.; Klee, D.; Hocker, H., Chemical Vapour Deposition Polymerization of Substituted [2.2]Paracyclophanes. *Macromol. Rapid Commun.* **1998,** *19* (9), 441-444.

4. Nishino, T.; Meguro, M.; Nakamae, K.; Matsushita, M.; Ueda, Y., The Lowest Surface Free Energy Based on -Cf3 Alignment. *Langmuir* **1999,** *15* (13), 4321-4323.

5. Decher, G., Fuzzy Nanoassemblies: Toward Layered Polymeric Multicomposites. *Science* **1997,** *277* (5330), 1232-1237.

6. Roberts, G. G., Langmuir-Blodgett Films. *Contemp. Phys.* **1984,** *25* (2), 109-128.

7. Shimomura, A.; Nishino, T.; Maruyama, T., Display of Amino Groups on Substrate Surfaces by Simple Dip-Coating of Methacrylate-Based Polymers and Its Application to DNA Immobilization. *Langmuir* **2013,** *29* (3), 932-938.

8. Yamamoto, S.; Kitahata, S.; Shimomura, A.; Tokuda, K.; Nishino, T.; Maruyama, T., Surfactant-Induced Polymer Segregation to Produce Antifouling Aurfaces Via Dip-Coating with an Amphiphilic Polymer. *Langmuir* **2015,** *31* (1), 125-131.

9. Hara, M.; Kitahata, S.; Nishimori, K.; Miyahara, K.; Morita, K.; Tokuda, K.; Nishino, T.; Maruyama, T., Surface-Functionalization of Isotactic Polypropylene Via Dip-Coating with a Methacrylate-Based Terpolymer Containing Perfluoroalkyl Groups and Poly(Ethylene Glycol). *Polym. J.* **2019,** *51* (5), 489-499.

10. Nishimori, K.; Kitahata, S.; Nishino, T.; Maruyama, T., Controlling Surface-Segregation of a Polymer to Display Carboxy Groups on an Outermost Surface Using Perfluoroacyl Group. *Langmuir* **2018,** *34*, 6396-6404.

11. Gevrek, T. N.; Ozdeslik, R. N.; Sahin, G. S.; Yesilbag, G.; Mutlu, S.; Sanyal, A., Functionalization of Reactive Polymeric Coatings Via Diels-Alder Reaction Using Microcontact Printing. *Macromol. Chem. Phys.* **2012,** *213* (2), 166-172.

12. Harris, L. G.; Schofield, W. C. E.; Doores, K. J.; Davis, B. G.; Badyal, J. P. S., Rewritable Glycochips. *J. Am. Chem. Soc.* **2009,** *131* (22), 7755-7761.

13. Roucoules, V.; Schofield, W. C. E.; Badyal, J. P. S., Photo-Rewritable Molecular Printing. *J. Mater. Chem.* **2011,** *21* (40), 16153-16161.

14. Roling, O.; De Bruycker, K.; Vonhoren, B.; Stricker, L.; Korsgen, M.; Arlinghaus, H. F.; Ravoo, B. J.; Du Prez, F. E., Rewritable Polymer Brush Micropatterns Grafted by Triazolinedione Click Chemistry. *Angew. Chem. Int. Ed.* **2015,** *54* (44), 13126-13129.

15. Du, X.; Li, J. S.; Welle, A.; Li, L. X.; Feng, W. Q.; Levkin, P. A., Reversible and Rewritable Surface Functionalization and Patterning Via Photodynamic Disulfide Exchange. *Adv. Mater.* **2015,** *27* (34), 4997-5001.

16. Goss, K. U.; Bronner, G., What Is So Special About the Sorption Behavior of Highly Fluorinated Compounds? *J. Phys. Chem. A* **2006,** *110* (30), 9518-9522.

17. Huque, F. T. T.; Jones, K.; Saunders, R. A.; Platts, J. A., Statistical and Theoretical Studies of Fluorophilicity. *J. Fluorine Chem.* **2002,** *115* (2), 119-128.

18. Beier, P.; O'Hagan, D., Enantiomeric Partitioning Using Fluorous Biphase Methodology for Lipase-Mediated (Trans)Esterifications. *Chem. Commun.* **2002,** (16), 1680-1681.

19. Hungerhoff, B.; Sonnenschein, H.; Theil, F., Separation of Enantiomers by Extraction Based on Lipase-Catalyzed Enantiomer-Selective Fluorous-Phase Labeling. *Angew. Chem. Int. Ed.* **2001,** *40* (13), 2492-2494.

20. Maruyama, T.; Nakashima, K.; Kubota, F.; Goto, M., Perfluorocarbon-Based Liquid-Liquid Extraction for Separation of Transition Metal Ions. *Anal. Sci.* **2007,** *23* (7), 763-765.

21. Studer, A.; Hadida, S.; Ferritto, R.; Kim, S. Y.; Jeger, P.; Wipf, P.; Curran, D. P., Fluorous Synthesis: A Fluorous-Phase Strategy for Improving Separation Efficiency in Organic Synthesis. *Science* **1997,** *275* (5301), 823-826.

22. Zhang, W., Fluorous Synthesis of Heterocyclic Systems. *Chem. Rev.* **2004,** *104* (5), 2531-2556.

23. Brittain, S. M.; Ficarro, S. B.; Brock, A.; Peters, E. C., Enrichment and Analysis of Peptide Subsets Using Fluorous Affinity Tags and Mass Spectrometry. *Nat. Biotechnol.* **2005,** *23* (4), 463-468.

24. de Visser, P. C.; van Helden, M.; Filippov, D. V.; van der Marel, G. A.; Drijfhout, J. W.; van Boom, J. H.; Noort, D.; Overkleeft, H. S., A Novel, Base-Labile Fluorous Amine Protecting Group: Synthesis and Use as a Tag in the Purification of Synthetic Peptides. *Tetrahedron Lett.* **2003,** *44* (50), 9013-9016.

25. Chen, G. S.; Pohl, N. L., Synthesis of Fluorous Tags for Incorporation of Reducing Sugars into a Quantitative Microarray Platform. *Org. Lett.* **2008,** *10* (5), 785-788.

26. Vegas, A. J.; Fuller, J. H.; Koehler, A. N., Small-Molecule Microarrays as Tools in Ligand Discovery. *Chem. Soc. Rev.* **2008,** *37* (7), 1385-1394.

27. Wang, D.; Oleschuk, R. D.; Horton, J. H., Surface Modification of Poly(Dimethylsiloxane) with a Perfluorinated Alkoxysilane for Selectivity toward Fluorous Tagged Peptides. *Langmuir* **2008,** *24* (3), 1080-1086.

28. Santos, C. M.; Kumar, A.; Zhang, W.; Cai, C. Z., Functionalization of Fluorous Thin Films Via "Click" Chemistry. *Chem. Commun.* **2009,** (20), 2854-2856.

29. Santos, C. M.; Kumar, A.; Kolar, S. S.; Contreras-Caceres, R.; McDermott, A.; Cai, C. Z., Immobilization of Antimicrobial Peptide Ig-25 onto Fluoropolymers Via Fluorous Interactions and Click Chemistry. *ACS Appl. Mater. Interfaces* **2013,** *5* (24), 12789-12793.

30. Mamidyala, S. K.; Ko, K. S.; Jaipuri, F. A.; Park, G.; Pohl, N. L., Noncovalent Fluorous Interactions for the Synthesis of Carbohydrate Microarrays. *J. Fluorine Chem.* **2006,** *127* (4-5), 571-579.

31. Ko, K. S.; Jaipuri, F. A.; Pohl, N. L., Fluorous-Based Carbohydrate Microarrays. *J. Am. Chem. Soc.* **2005,** *127* (38), 13162-3.

32. Brady, J. R. F.; Ed., S. J., Mordern Fluoropolymers. *John Wiley & Sons* **1997**.

33. Zhao, Z. L.; Ni, H. G.; Han, Z. Y.; Jiang, T. F.; Xu, Y. J.; Lu, X. L.; Ye, P., Effect of Surface Compositional Heterogeneities and Microphase Segregation of Fluorinated Amphiphilic Copolymers on Antifouling Performance. *ACS Appl. Mater. Interfaces* **2013,** *5* (16), 7808-7818.

34. Nicholson, R. L.; Ladlow, M. L.; Spring, D. R., Fluorous Tagged Small Molecule Microarrays. *Chem. Commun.* **2007,** (38), 3906-3908.

35. Flynn, G. E.; Withers, J. M.; Macias, G.; Sperling, J. R.; Henry, S. L.; Cooper, J. M.; Burley, G. A.; Clark, A. W., Reversible DNA Micro-Patterning Using the Fluorous Effect. *Chem. Commun.* **2017,** *53* (21), 3094-3097.

36. Huang, W. G.; Proctor, A.; Sims, C. E.; Allbritton, N. L.; Zhang, Q. S., Fluorous Enzymatic Synthesis of Phosphatidylinositides. *Chem. Commun.* **2014,** *50* (22), 2928-2931.

37. Li, B. Y.; Juang, D. S.; Adak, A. K.; Hwang, K. C.; Lin, C. C., Fabrication of a Protein Microarray by Fluorous-Fluorous Interaction. *Sci. Rep.* **2017,** *7*, Article number 7053.

38. Sun, F.; Castner, D. G.; Mao, G.; Wang, W.; McKeown, P.; Grainger, D. W., Spontaneous Polymer Thin Film Assembly and Organization Using Mutually Immiscible Side Chains. *J. Am. Chem. Soc.* **1996,** *118* (8), 1856-1866.

39. Hirao, A.; Sugiyama, K.; Yokoyama, H., Precise Synthesis and Surface Structures of Architectural Per- and Semifluorinated Polymers with Well-Defined Structures. *Prog. Polym. Sci.* **2007,** *32* (12), 1393-1438.

40. Koda, Y.; Terashima, T.; Sawamoto, M., Multimode Self-Folding Polymers Via Reversible and Thermoresponsive Self-Assembly of Amphiphilic/Fluorous Random Copolymers. *Macromolecules* **2016,** *49* (12), 4534-4543.

41. Bae, K. J.; Yao, W. H.; He, Y. L.; Cho, Y. R., Wetting Behavior of Liquids on Micro-Patterned Polymer Surfaces Fabricated by Thermal Imprinting. *Korean J. Met. Mater.* **2017,** *55* (9), 624-631.

42. Yao, W. H.; Li, L.; Li, O. L.; Cho, Y. W.; Jeong, M. Y.; Cho, Y. R., Robust, Self-Cleaning, Amphiphobic Coating with Flower-Like Nanostructure on Micro-Patterned Polymer Substrate. *Chem. Eng. J.* **2018,** *352*, 173-181.

43. van de Grampel, R. D.; Ming, W.; Gildenpfennig, A.; Laven, J.; Brongersma, H. H.; de With, G.; van der Linde, R., Quantification of Fluorine Density in the Outermost Atomic Layer. *Langmuir* **2004,** *20* (1), 145-149.

44. de Grampel, R. D. V.; Ming, W.; Gildenpfennig, A.; van Gennip, W. J. H.; Laven, J.; Niemantsverdriet, J. W.; Brongersma, H. H.; de With, G.; van der Linde, R., The Outermost Atomic Layer of Thin Films of Fluorinated Polymethacrylates. *Langmuir* **2004,** *20* (15), 6344-6351.

45. Wong, D. A.; O'Rourke-Muisener, P. A. V.; Koberstein, J. T., Effect of Chain Architecture on Surface Segregation in Functional Polymers: Synthesis and Surface Properties of End- and Center-Functional Poly(D,L-Lactide). *Macromolecules* **2007,** *40* (5), 1604-1614.

46. Hennig, A.; Borcherding, H.; Jaeger, C.; Hatami, S.; Wurth, C.; Hoffmann, A.; Hoffmann, K.; Thiele, T.; Schedler, U.; Resch-Genger, U., Scope and Limitations of Surface Functional Group Quantification Methods: Exploratory Study with Poly(Acrylic Acid)-Grafted Micro- and Nanoparticles. *J. Am. Chem. Soc.* **2012,** *134* (19), 8268-8276.

47. Lindner, E., A Low Surface Free Energy Approach in the Control of Marine Biofouling. *Biofouling* **1992,** *6* (2), 193-205.

48. Tamada, Y.; Ikada, Y., Effect of Preadsorbed Proteins on Cell-Adhesion to Polymer Surfaces. *J. Colloid Interface Sci.* **1993,** *155* (2), 334-339.

49. Johnson, J. K.; Hoffman, C. M.; Smith, D. A.; Xia, Z. Y., Advanced Filtration Membranes for the Removal of Perfluoroalkyl Species from Water. *Acs Omega* **2019,** *4* (5), 8001-8006.

50. Glatz, H.; Blay, C.; Engelhardt, H.; Bannwarth, W., New Fluorous Reversed Phase Silica Gels for Hplc Separations of Perfluorinated Compounds. *Chromatographia* **2004,** *59* (9-10), 567-570.

51. Kumar, A.; Whitesides, G. M., Features of Gold Having Micrometer to Centimeter Dimensions Can Be Formed through a Combination of Stamping with an Elastomeric Stamp and an Alkanethiol Ink Followed by Chemical Etching. *Appl. Phys. Lett.* **1993,** *63* (14), 2002-2004.

52. Michel, B.; Bernard, A.; Bietsch, A.; Delamarche, E.; Geissler, M.; Juncker, D.; Kind, H.; Renault, J. P.; Rothuizen, H.; Schmid, H.; SchmidtWinkel, P.; Stutz, R.; Wolf, H., Printing

Meets Lithography: Soft Approaches to High-Resolution Patterning (vol 45, pg 697, 2001). *IBM Journal of Research and Development* **2001,** *45* (6), 870-870.

53. Xia, Y. N.; Whitesides, G. M., Soft Lithography. *Angew. Chem. Int. Ed.* **1998,** *37* (5), 550-575.

TOC entry

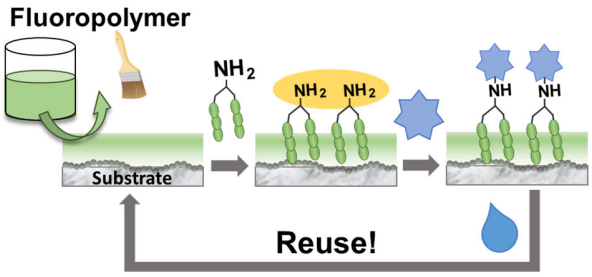

Supporting Information

A rewritable surface on a plastic substrate using fluorous affinity

*Takane Tsuchii,[†] Kazuki Kaneko,[†] Kenta Morita,[†] Takashi Nishino,[†] Tatsuo Maruyama[†,‡,]**

[†] Department of Chemical Science and Engineering, Graduate School of Engineering, Kobe University, 1-1 Rokkodai, Nada-ku, Kobe 657-8501, Japan.

[‡] Research Center for Membrane and Film Technology, Kobe University, 1-1 Rokkodai, Nada, Kobe 657-8501, Japan

*Corresponding author

tmarutcm@crystal.kobe-u.ac.jp

Experimental details

Materials

The acrylic (poly(methyl methacrylate); PMMA) substrate (0.5-mm-thick) was purchased from Nitto Jushi Kogyo Co., Ltd. (Tokyo, Japan). Methyl methacrylate (MMA), 2,2-azobisisobutyronitrile (AIBN) and 2-(perfluorohexyl)ethyl acrylate (PFEA6) were purchased from Wako Pure Chemical Industries, Inc. (Osaka, Japan). 2-(Perfluorooctyl)ethyl acrylate (PFEA8) was provided by DIC Corp. (Tokyo, Japan). 1H,1H-Perfluorononylamine (Rf8-NH_2) was purchased from Sigma Aldrich (St. Louis, MO). Sulfo-Cy5-NHS ester was purchased from Lumiprobe Corporation (Hunt Valley, MD). Boc-Glu-OH was purchased from Watanabe Chemical Co., Ltd. (Hiroshima, Japan). 1H,1H-Perfluoroheptylamine (Rf6-NH_2) was purchased from Combi-Blocks, Inc (San Diego, CA). 4-(4,6-Dimethoxy-1,3,5-triazin-2-yl)-4-methylmorpholinium chloride (DMT-MM), biotin, and 2-(perfluorobutyl)ethyl acrylate (PFEA4) were purchased from Tokyo Chemical Industry Co., Ltd. (Tokyo, Japan). 1H,1H-Perfluoropentylamine (Rf4-NH_2) was purchased from Fluoro Chem (Derbyshire, UK). Acrylate monomers and fluorous acrylate monomers were distilled under reduced pressure before use or a polymerization inhibitor was removed using an inhibitor-removing column. 1-Ethyl-3-(3-dimethylaminopropyl) carbodiimide, hydrochloride (WSC) was purchased from Dojindo Molecular Technologies Inc. (Kumamoto, Japan). Streptavidin Fluor™ 488 conjugate was provided by Thermo Fisher Scientific (Waltham, MA). All other chemicals were purchased from Wako Pure Chemical Industries and were used as received. The water used was high-quality

deionized water (Milli-Q water, >15 MΩ cm), produced using a Milli-Q Integral 3 system (Millipore, Molsheim, France).

Table S1. Amounts of reagents used for the polymerization of PF8-(X:Y), PF6-(6:4), and PF4-(6:4).

Polymer	MMA (g)	Rf-acrylate (g)	AIBN (mg)	Ethyl acetate (mL)	Vial size (mL)
PF8-(9:1)	3.0	1.8	23	20	50
PF8-(8:2)	2.5	3.2	29	20	50
PF8-(7:3)	3.5	7.8	51	25	50
PF8-(6:4)	1.5	5.3	34	20	50
PF8-(5:5)	1.0	5.2	31	20	50
PF6-(6:4)	1.0	2.8	20	15	50
PF4-(6:4)	1.0	2.1	16	7	20

Synthesis of $(Rf6)_2$-NH_2

Scheme S1. Synthesis of $(Rf6)_2$-NH_2.

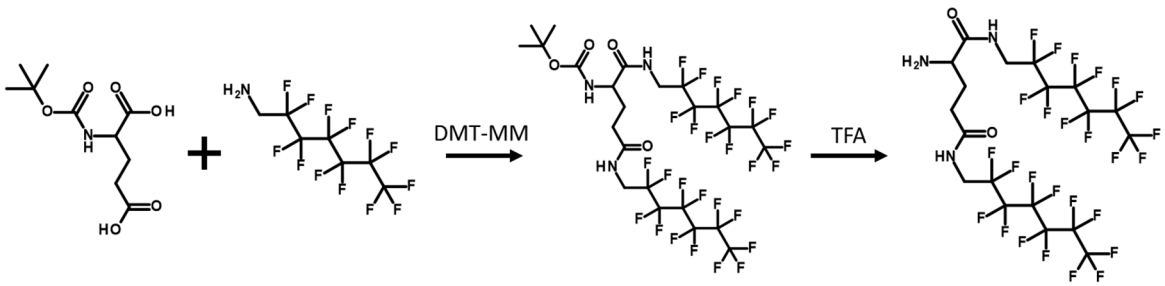

Boc-Glu-OH (0.18 mmol) was dissolved in 2 mL methanol. 1H,1H-Perfluoroheptylamine (Rf6-NH_2) (0.36 mmol) was dissolved in 2 mL methanol. These solutions were mixed in a 20-mL vial. DMT-MM (0.39 mmol) was added to the mixture and gently stirred at room temperature overnight,

followed by solvent evaporation at 60 °C. The resulting dry residue was dissolved in THF and the remaining DMT-MM was removed by filtration. The solvent was then evaporated at 60 °C, and the dry residue was dissolved in 6 mL dichloromethane. The dichloromethane solution (6 mL), a 2 wt.% Na_2CO_3 aqueous solution (3 mL), and methanol (1.5 mL) were added to a separating funnel and mixed well. The dichloromethane phase was collected and evaporated. The precipitate in the vial was dissolved in 0.6 mL methanol at 60 °C. The solution was cooled on ice, and the precipitate was collected. The precipitate was dissolved in 2 mL dichloromethane, and 150 μL trifluoroacetic acid (TFA) was added to deprotect the *tert*-butoxycarbonyl groups. The dichloromethane phase was evaporated, and the product ($(Rf6)_2$-NH_2) was freeze dried. This product was analyzed by ^{1}H-NMR and matrix-assisted laser desorption ionization time-of-flight mass spectrometry (MALDI TOF-MS) using an ultrafleXtreme mass spectrometer (Bruker, Billerica, MA). The ^{1}H-NMR and MALDI TOF-MS results are shown in Figure S9 and S10. Yield: 73%.

Synthesis of $(Rf4)_2$-NH_2

Scheme S2. Synthesis of $(Rf4)_2$-NH_2.

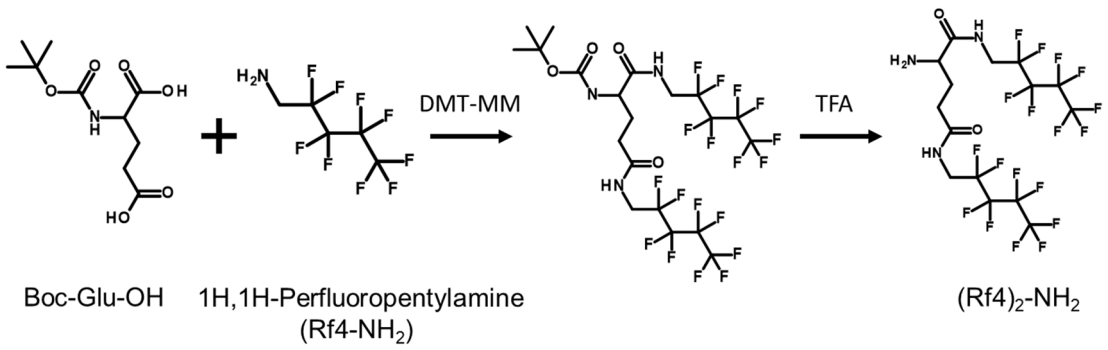

$(Rf4)_2$-NH_2 was synthesized in a similar manner to $(Rf6)_2$-NH_2; Yield = 34%; ^{1}H-NMR and MALDI TOF-MS results are shown in Figure S11 and S12.

Synthesis of $(Rf6)_2$-biotin

Scheme S3. Synthesis of $(Rf6)_2$-biotin.

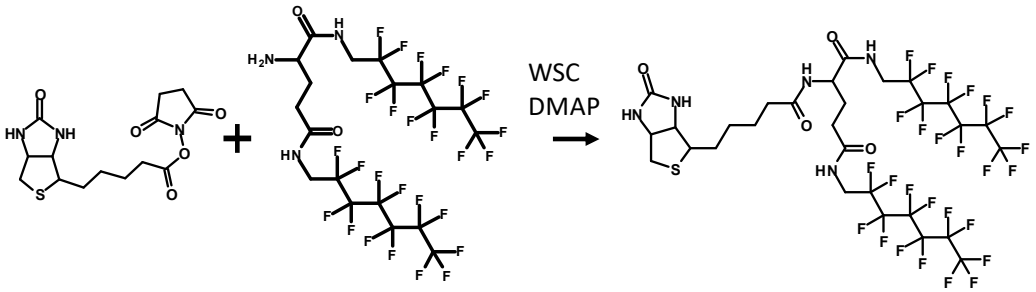

Biotin $(Rf6)_2$-NH_2 $(Rf6)_2$-biotin

Biotin (30.5 mmol), $(Rf6)_2$-NH_2 (31.5 mmol), 1-ethyl-3-(3-dimethylaminopropyl)carbodiimide, hydrochloride (WSC; 33.4 mmol), and 4-dimethylaminopyridine (DMAP; 33.4 mmol) were dissolved in 1.8 mL *N,N*-dimethylformamide (DMF) and mixed overnight at 37 °C, followed by evaporation of the DMF. The residue was washed with water three times, and the product was obtained as a white powder after lyophilization of the residue. The product was analyzed by ^{1}H-NMR and MALDI-TOF MS (Figure S13 and S14); Yield = 39%.

Results

Table S2. Number-averaged molecular weights, polydispersity indices, and exact copolymerization ratio of PFn-(6:4).

Polymer	Monomer ratio in a product	*M*n	*M*w/*M*n
PF8-(6:4)	58:42	3.1×10^4	1.4
PF6-(6:4)	62:38	5.8×10^4	1.3
PF4-(6:4)	64:36	7.8×10^4	1.1

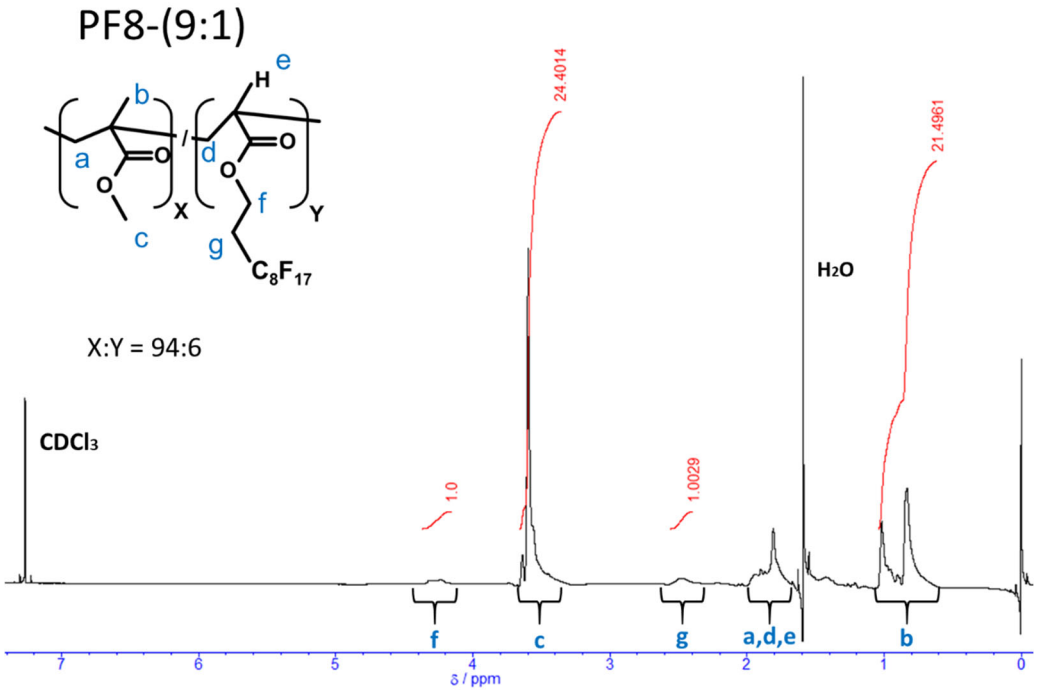

Figure S1. ^{1}H-NMR spectrum of PF8-(9:1).

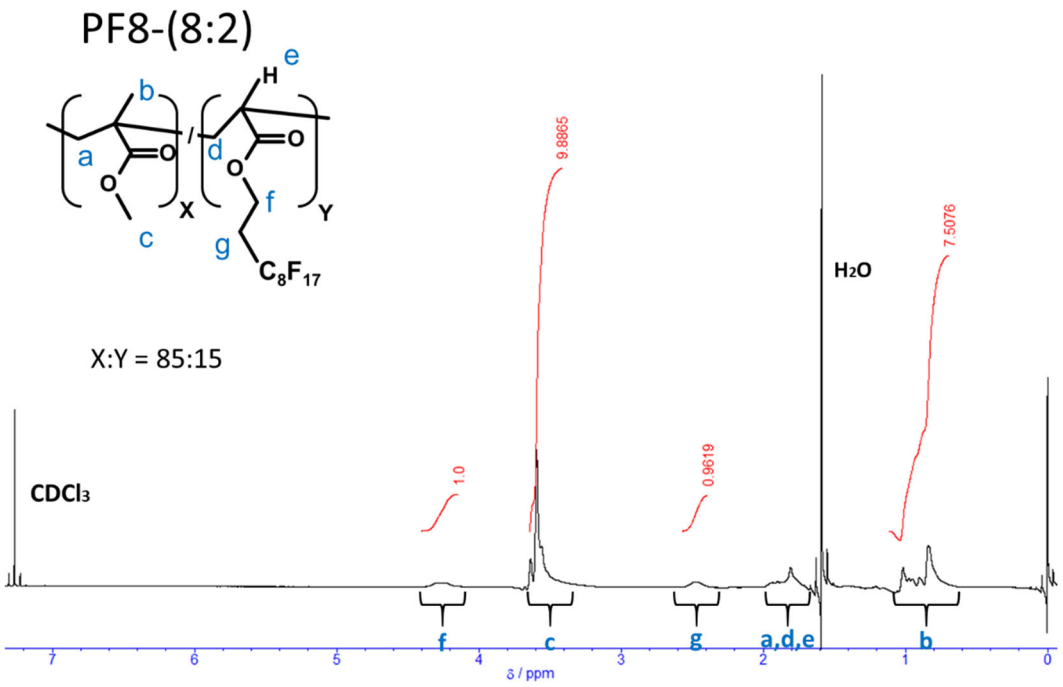

Figure S2. ^{1}H-NMR spectrum of PF8-(8:2).

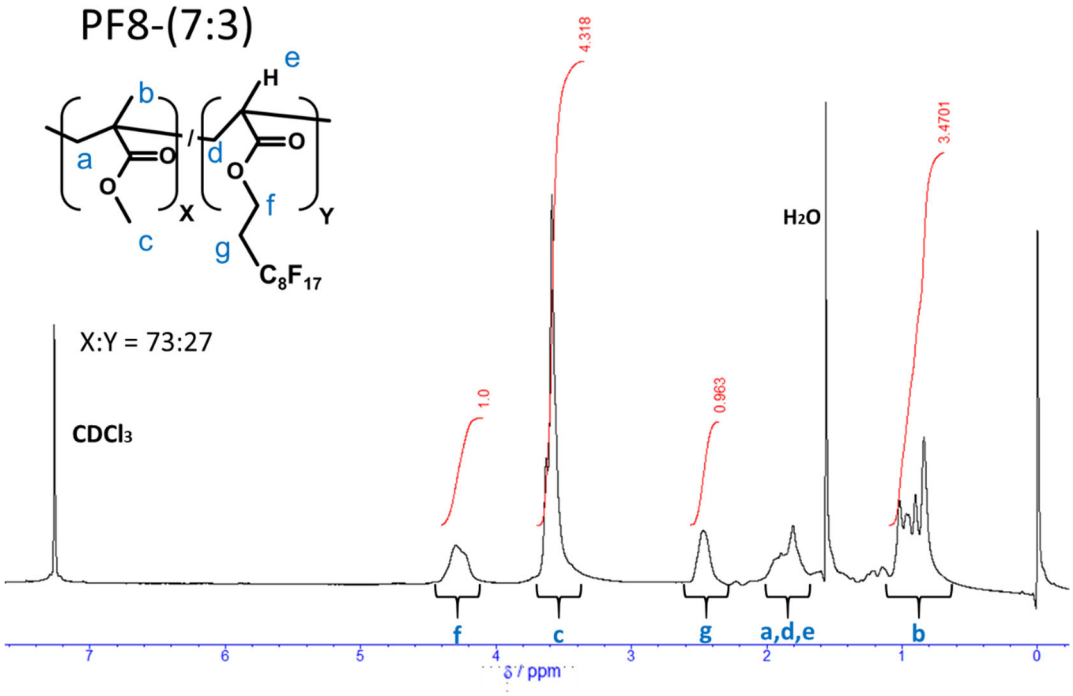

Figure S3. ^{1}H-NMR spectrum of PF8-(7:3).

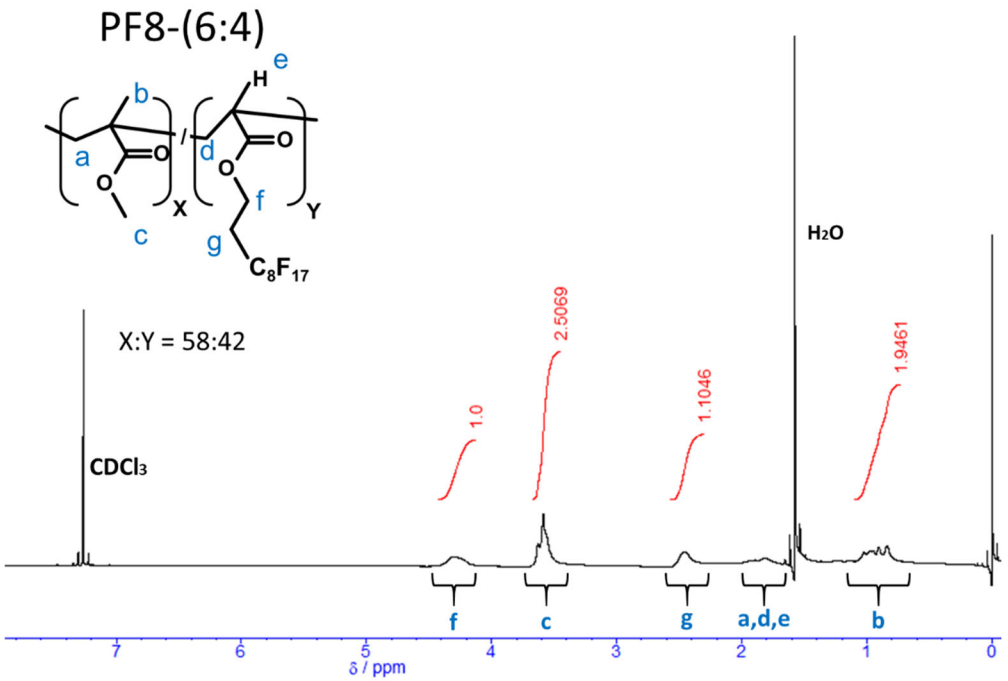

Figure S4. ^{1}H-NMR spectrum of PF8-(6:4).

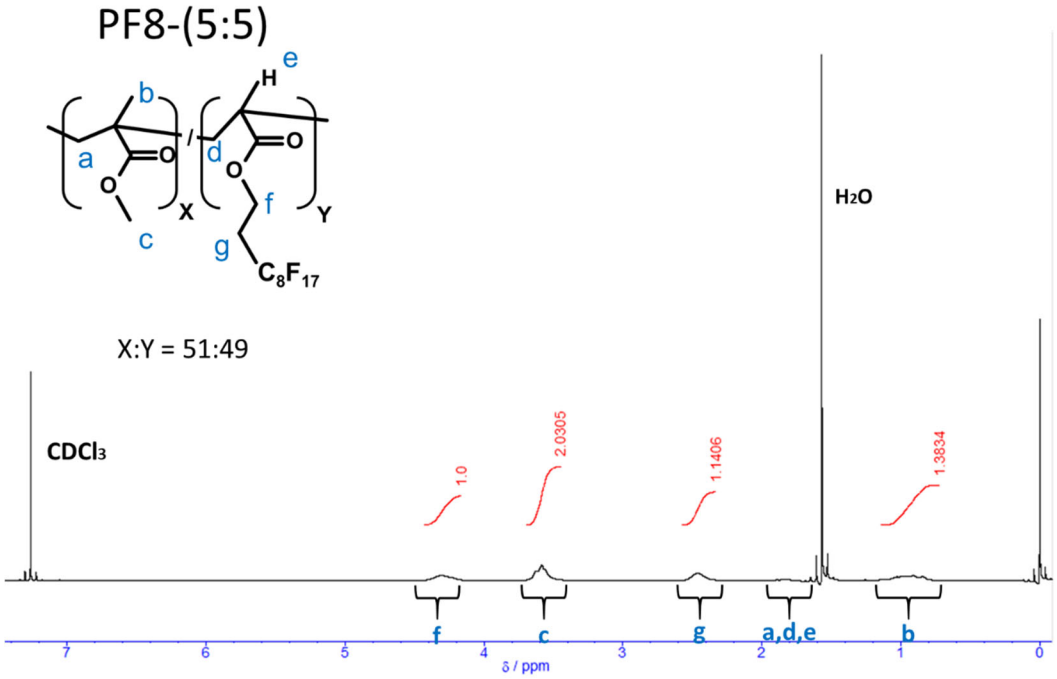

Figure S5. ^{1}H-NMR spectrum of PF8-(5:5).

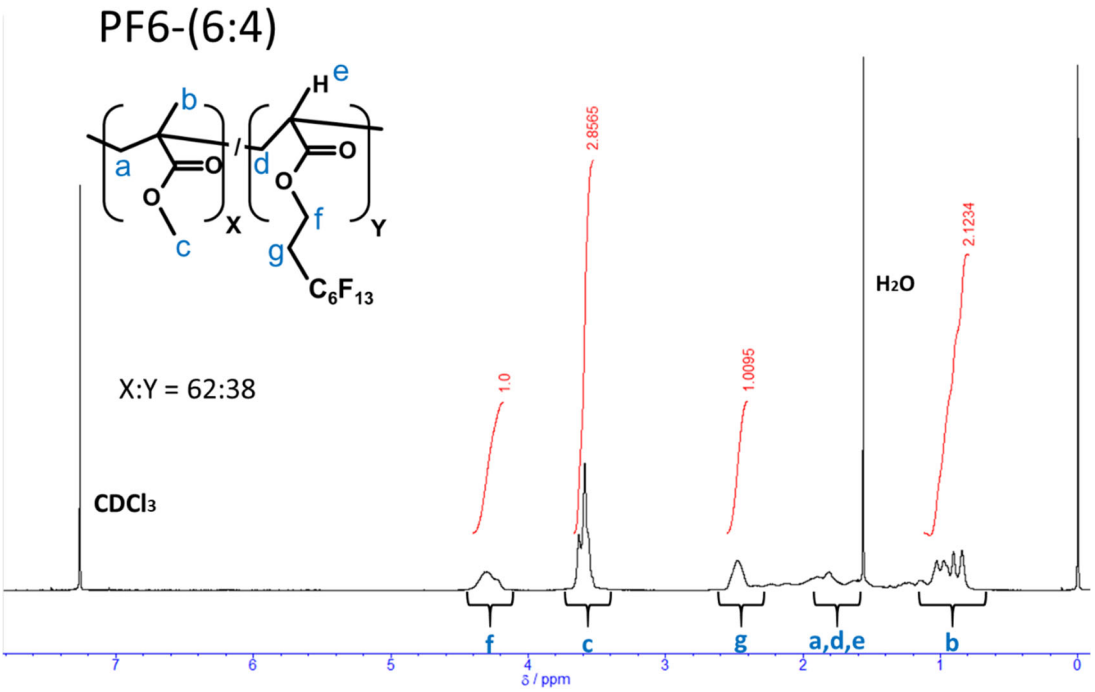

Figure S6. ^{1}H-NMR spectrum of PF6-(6:4).

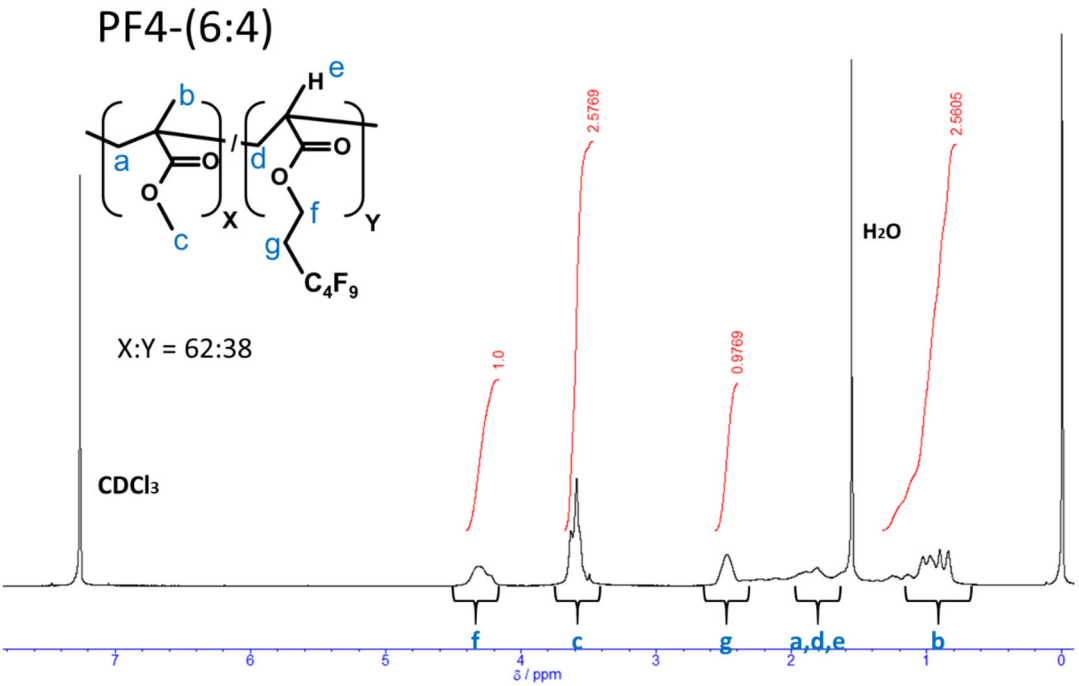

Figure S7. ^{1}H-NMR spectrum of PF4-(6:4).

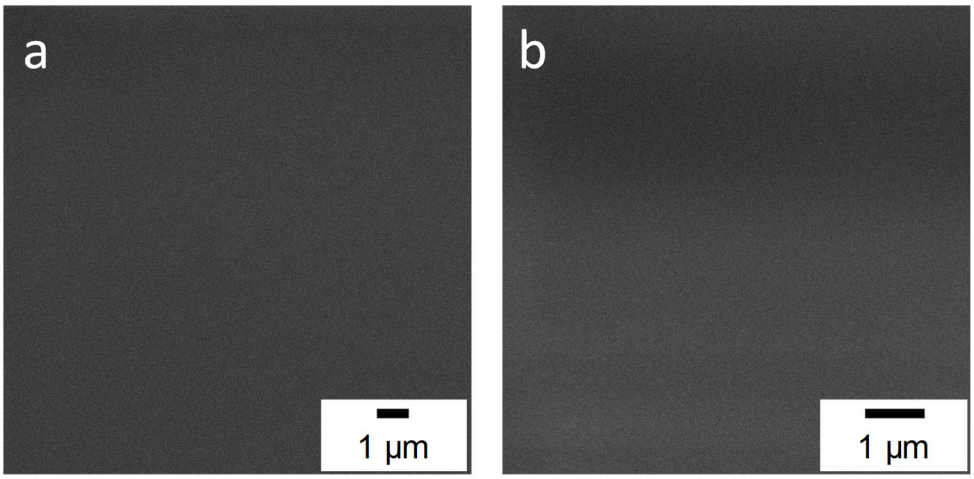

Figure S8. FE-SEM images of (a) a bare PMMA surface and (b) a PF8-(6:4)-coated surface.

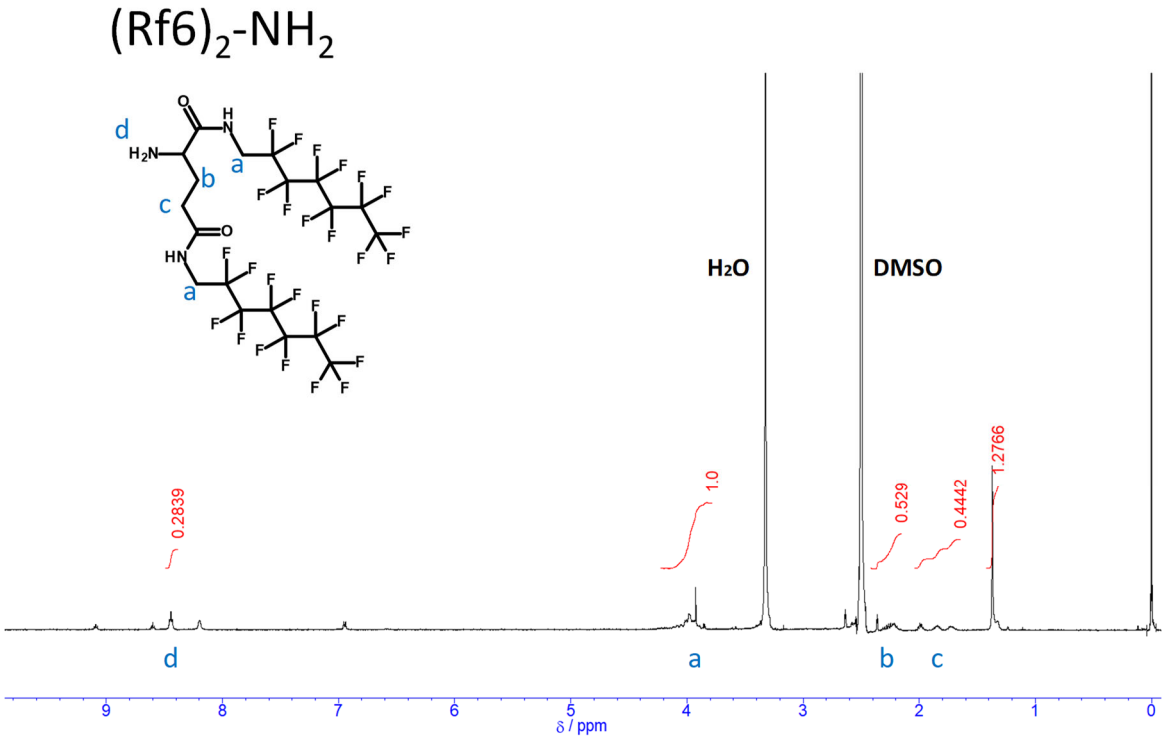

Figure S9. ^{1}H-NMR spectrum of (Rf6)$_2$-NH$_2$.

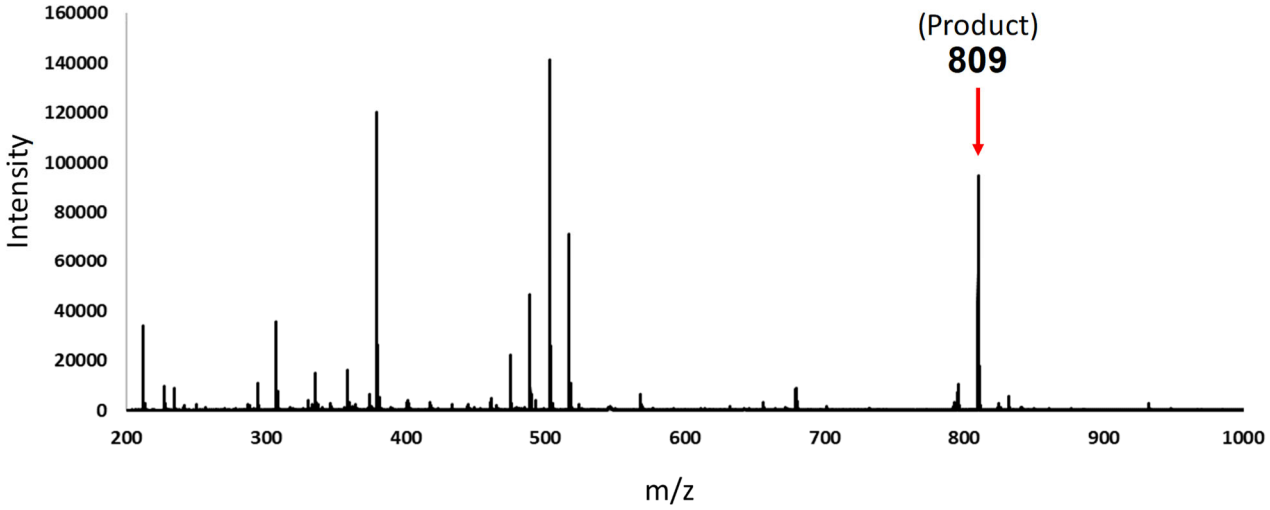

Figure S10. MALDI-TOF MS chart of $(Rf6)_2$-NH_2.

MAIDI-TOF MS (m/z): $[M + H]^+$ calcd for $C_{19}H_{14}F_{26}N_3O_2$ = 810.1; found = 810.1.

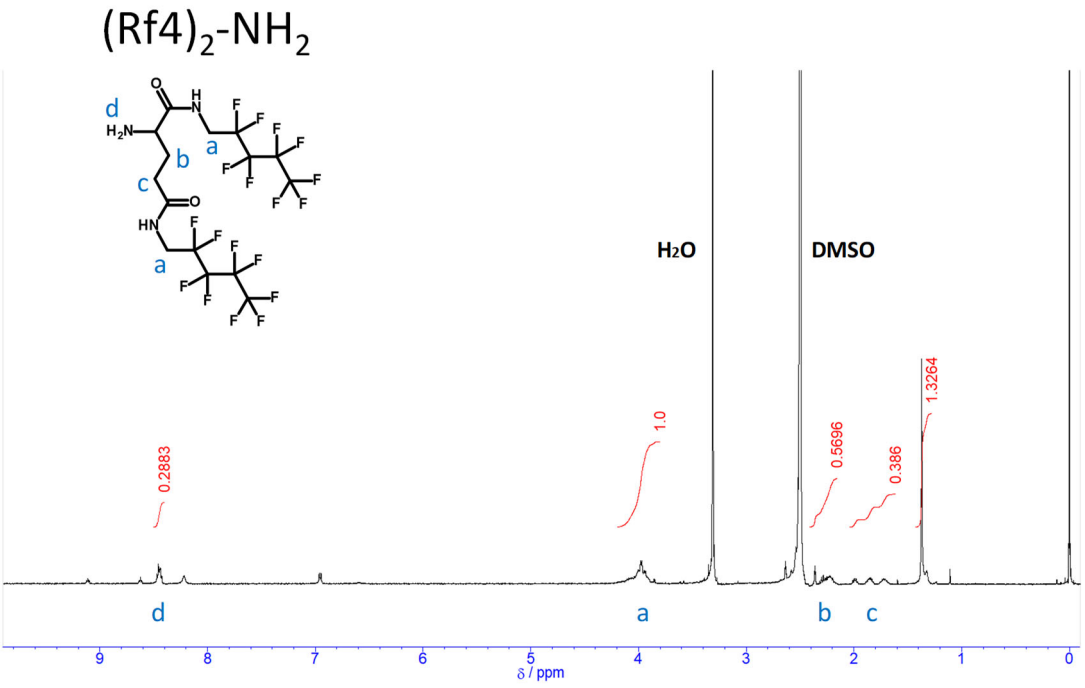

Figure S11. ^{1}H-NMR spectrum of $(Rf4)_2$-NH_2.

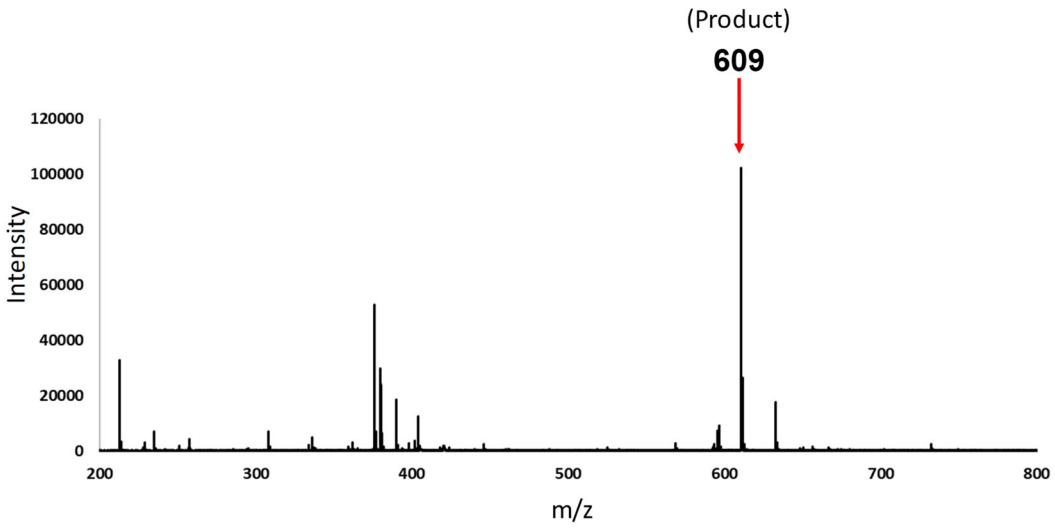

Figure S12. MALDI-TOF MS chart of $(Rf4)_2$-NH_2.

MAIDI-TOF MS (m/z): $[M + H]^+$ calcd for $C_{15}H_{14}F_{18}N_3O_2$ = 610.1; found = 610.7.

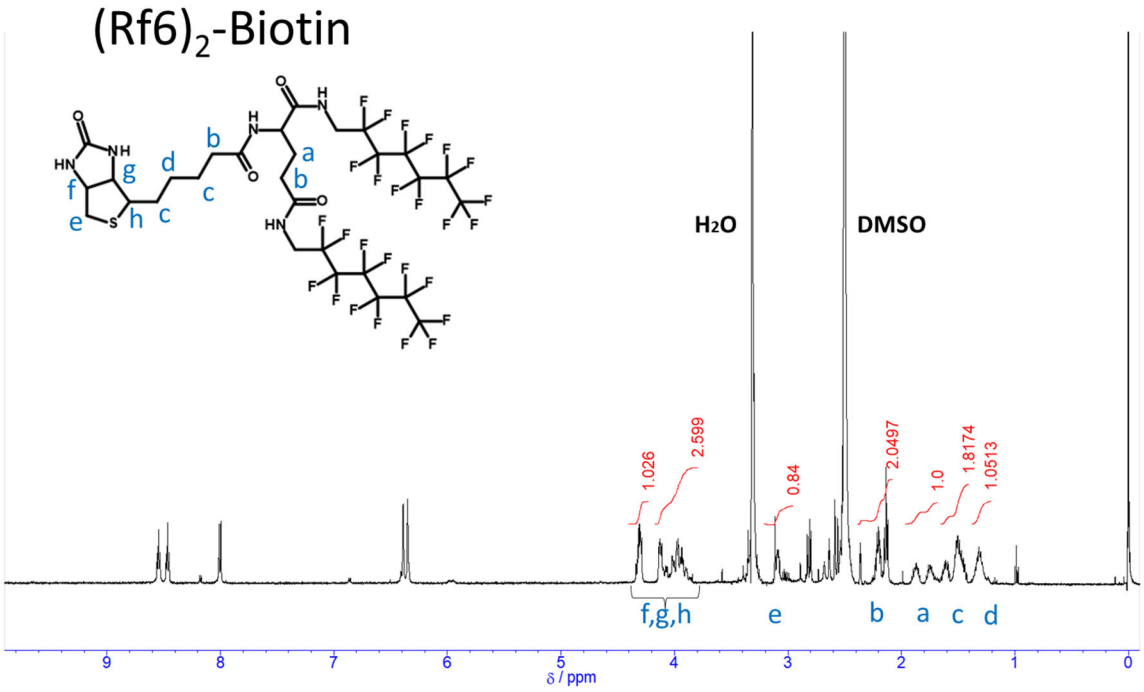

Figure S13. ^{1}H-NMR spectrum of $(Rf6)_2$-biotin.

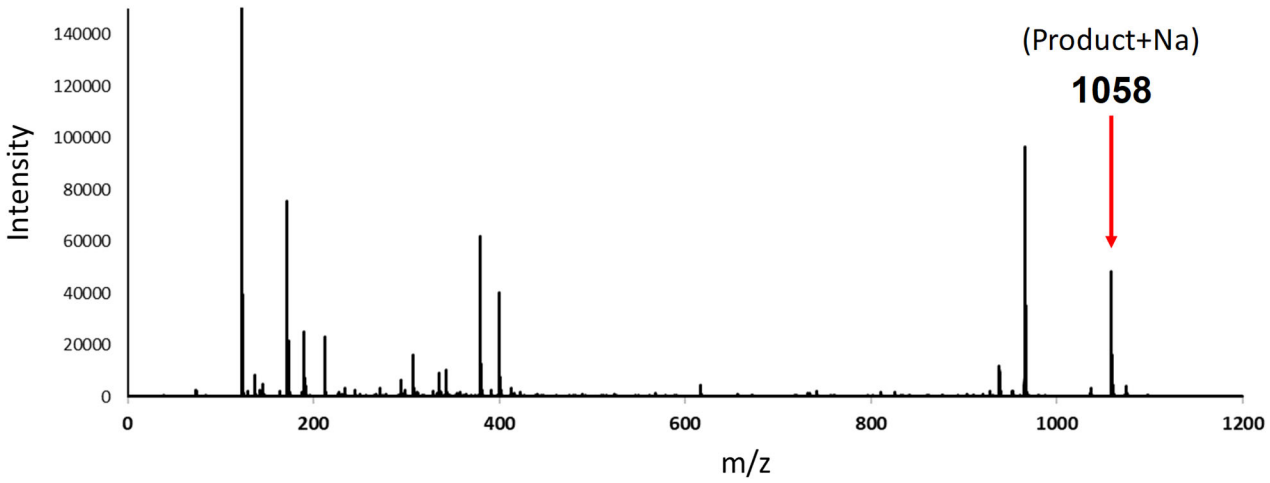

Figure S14. MALDI-TOF MS chart of $(Rf6)_2$-biotin.

MAIDI-TOF MS (m/z): $[M + Na]^+$ calcd for $C_{29}H_{27}F_{26}N_5O_4SNa$ = 1058.1; found = 1058.3.

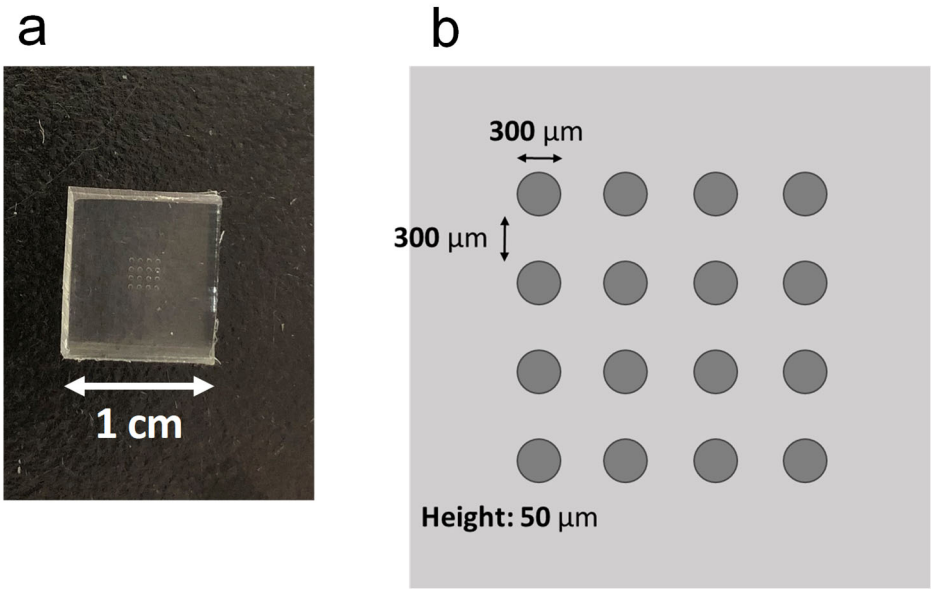

Figure S15. a) Optical image of a PDMS stamp; b) illustration of the geometry of a PDMS stamp.